Photoactivation of diiodido-Pt(IV) complexes coupled to upconverting nanoparticles

Stefanie Perfahl,[a] *Marta M. Natile,*[b] *Heba S. Mohamad,*[c] *Christiane A. Helm,*[c] *Carola Schulzke,*[d] *Giovanni Natile,*[e] *Patrick J. Bednarski*[a*]

[a)] Institute of Pharmacy, Ernst-Moritz-Arndt University of Greifswald, 17487 Greifswald, Germany

[b)] CNR-ICMATE, Department of Chemical Sciences, University of Padova, 35131 Padova, Italy

[c)] Institute of Physics, Ernst-Moritz-Arndt University of Greifswald, 17487 Greifswald, Germany

[d)] Institute of Biochemistry, Ernst-Moritz-Arndt University of Greifswald, 17489 Greifswald, Germany

[e)] Department of Chemistry, University of Bari, 70125 Bari, Italy

bednarsk@uni-greifswald.de

Abstract. The preparation, characterization and surface modification of upconverting lanthanide-doped hexagonal $NaGdF_4$ nanocrystals attached to light sensitive diiodido-Pt(IV) complexes is presented. The evaluation for photoactivation and cytotoxicity of the novel carboxylated diiodido-Pt(IV) cytotoxic prodrugs by near infrared (NIR) light (λ = 980 nm) is also reported. We attempted two different strategies for attachment of light-sensitive diiodido-Pt(IV) complexes to Yb,Er- and Yb,Tm-doped β–$NaGdF_4$ upconverting nanoparticles (UCNPs) in order to provide nano-hybrids, which offer unique opportunities for selective drug activation within the tumor cells and subsequent spatio-temporal controlled drug release by NIR-to-visible light-upconversion: A) covalent attachment of the Pt(IV) complex via amide bond formation and B) carboxylate exchange of oleate on the surface of the UCNPs with diiodido-Pt(IV) carboxylato complexes. Initial feasibility studies showed that NIR applied by a 980 nm laser had only a slight effect on the stability of the various diiodido-Pt(IV) complexes but when UCNPs were present more rapid loss of the ligand-metal-charge-transfer (LMCT) bands of the diiodido-Pt(IV) complexes was observed. Furthermore, Pt released from the Pt(IV) complexes platinated calf-thymus DNA (ct-DNA) more rapidly when NIR was applied compared to dark controls. Of the two attachment strategies, method A with the covalently attached diiodido-Pt(IV) carboxylates via amide bond formation proved to be the most effective method for generating UCNPs that release Pt when irradiated with NIR; the released Pt was also able to bind irreversibly to calf thymus DNA. Nonetheless, only ca. 20% of the Pt on the surface of the UCNPs was in the Pt(IV) oxidation state, the rest was Pt(II), indicating chemical reduction of the diiodido-Pt(IV) prodrug by the UCNPs. Cytotoxicity studies with the various UCNP-Pt conjugates and constructs, tested on human leukemia HL60 cells in culture, indicated a substantial increase in cytotoxicity when

modified UCNPs were combined with 5 rounds of 30 min irradiation with NIR compared to dark controls, but NIR alone also had a significant cytotoxic effect at this duration.

Keywords. upconverting nanoparticles, photoactivatable Pt complexes, photoactivated chemotherapy, anticancer prodrug

Introduction

Photoactivated chemotherapy (PACT) has been attracting attention as a potential novel therapy of cancer because of the ability to selectively activate non-toxic prodrugs of anticancer agents by light in and around a localized tumor.[1] In particular, transition metal-based agents, such as diazido-Pt(IV) complexes, have been investigated for this strategy.[2-4] Recently, efforts have aimed at changing the pharmaceutical properties of such light-activatable Pt(IV) complexes to help improve their tumor selectivity and potency by attaching biologically active ligands to the Pt(IV) complex. For example, the photoactive *trans,trans,trans*-$[Pt(N_3)_2(OH)(succinato)(pyridine)_2]$ was coupled to either guanidinoneomycin[5] or to a cyclic peptide that is selectively recognized by cell surface integrins[6], thus facilitating tumor cell uptake of the Pt(IV) complex. To a cis-coordinated 2,2'-bipyridinodiazido-Pt(IV) complex, which is also light activatable, Kasparkova and coworkers coupled a histone deacetylase inhibitor via the trans-hydroxo ligands to improve cytotoxicity.[7]

Nevertheless, the need for relatively short wavelength light ($\lambda < 500$ nm) for activation of transition metal complexes to cytotoxic species limits wider applications with such diazido-Pt(IV) complexes because only superficial tumors are treatable due to the small penetration of

visible light into tissues.[8] By converting multiple longer wavelength photons (i.e., near-infrared photons) into one photon of shorter wavelength (i.e., visible light), upconverting nanoparticles (UCNPs) promise to overcome this problem.[9, 10] Thus, light of longer wavelength (e.g. λ = 980 nm) could penetrate deeper into tumor tissues than UV radiation, be upconverted by the nanoparticles to a higher energy photon that would activate a light-sensitive prodrug attached to the UCNPs, leading to the release of an active anticancer agent.

UCNP technologies are expanding rapidly in areas of biomedical imagining and drug delivery, as illustrated in a number of recent reviews.[9, 11, 12] Upconversion, also known as anti-Stokes emission, is a multiple photon process, whereby the sequential absorption of two or more photons by a material leads to the emission of a single photon of shorter wavelength.[13, 14] An UCNP is composed of an optically inert host matrix and optically active Ln^{3+} ions as luminescent centers. Among the possible host matrices, fluorides such as $NaGdF_4$ and $NaYF_4$ are often used due to their excellent chemical stability and low phonon energy (~ 350 cm^{-1}),[15] which limit deleterious non-radiative multi-photon relaxation pathway. $NaGdF_4$ and $NaYF_4$ UCNPs are known to crystallize in either cubic α-phase or hexagonal β-phase with the latter having upconversion emission an order of magnitude greater because of less symmetric lanthanide dopant sites. Concerning the optically active Ln^{3+} ions responsible of the upconversion emission, usually a sensitizer and at least one activator are embedded into the above host lattices by replacing gadolinium or yttrium cations. The best sensitizer for light at 980 nm is Yb^{3+} having a larger absorption cross-section among the Ln^{3+} ions. Moreover, the energy of excited state of Yb^{3+} is similar to those of Er^{3+}, Tm^{3+}, Ho^{3+} *etc*, thus facilitating efficient energy transfer from Yb^{3+} to other ions. Er^{3+}, Tm^{3+} and Ho^{3+} are the most used activators because of the ladder-like arrangement of their energy levels.[16] In this contribution, $NaGdF_4$:Yb,Er and $NaGdF_4$:Yb,Tm

with hexagonal β-phase which emit, respectively, in the visible and UV regions and in NIR, visible and UV regions, are considered.

Success with UCNPs coupled to photoactivatable prodrugs has recently been reported for two light activatable Pt(IV) anticancer prodrugs: diazido-Pt(IV)[17, 18] as well as a dichlorido-Pt(IV) complexes.[19] However, these Pt(IV) complexes only weakly absorb in the visible region of the spectrum. Here, we report on the development of photoactivatable diiodido-Pt(IV) diamines attached to UCNPs. Diiodido-Pt(IV) diamines were the first Pt complexes described that can be photoactivated with visible light to cytotoxic Pt(II) complexes,[20, 21] thus making them interesting candidates for UCNPs assisted PACT. It was anticipated that the intense ligand-to-metal charge-transfer (LMCT) bands of the diiodido-Pt(IV) diamines, that extend well into the visible region of the electromagnetic spectrum (i.e. up to λ = 500 nm), would overlap with emission bands of commonly used UCNPs. Thus, irradiation with NIR would induce emission of visible light from the UCNPs, causing photoreduction of the attached Pt(IV) prodrug to release a cytotoxic Pt(II) diamine.

One strategy to incorporate specific functionalities into Pt(IV) complexes is the use of Pt(IV) carboxylates as a design framework. In order to investigate the influence of various axial ligands on drug efficacies, Pt(IV) with functionalized carboxylate ligands were synthesized. We have evaluated two strategies for attaching diiodido-Pt(IV) diamines to Yb,Er(or Tm)-doped Gd-based UCNPs (Figure 1) and studied the effects of NIR on the release of Pt from these UCNPs as well as measured the binding of released Pt to DNA in a model system. Photoreduction of the kinetically inert Pt(IV) to a labile Pt(II) should then be followed by facile substitution of the carboxylate ligand for water and formation of the cytotoxic $[Ptx(H_2O)_2(en)]^{2+}$. Finally, the

cytotoxic actions of such modified UCNPs on human leukemia cancer cells in culture, with and without irradiation with NIR λ = 980 nm, have been investigated.

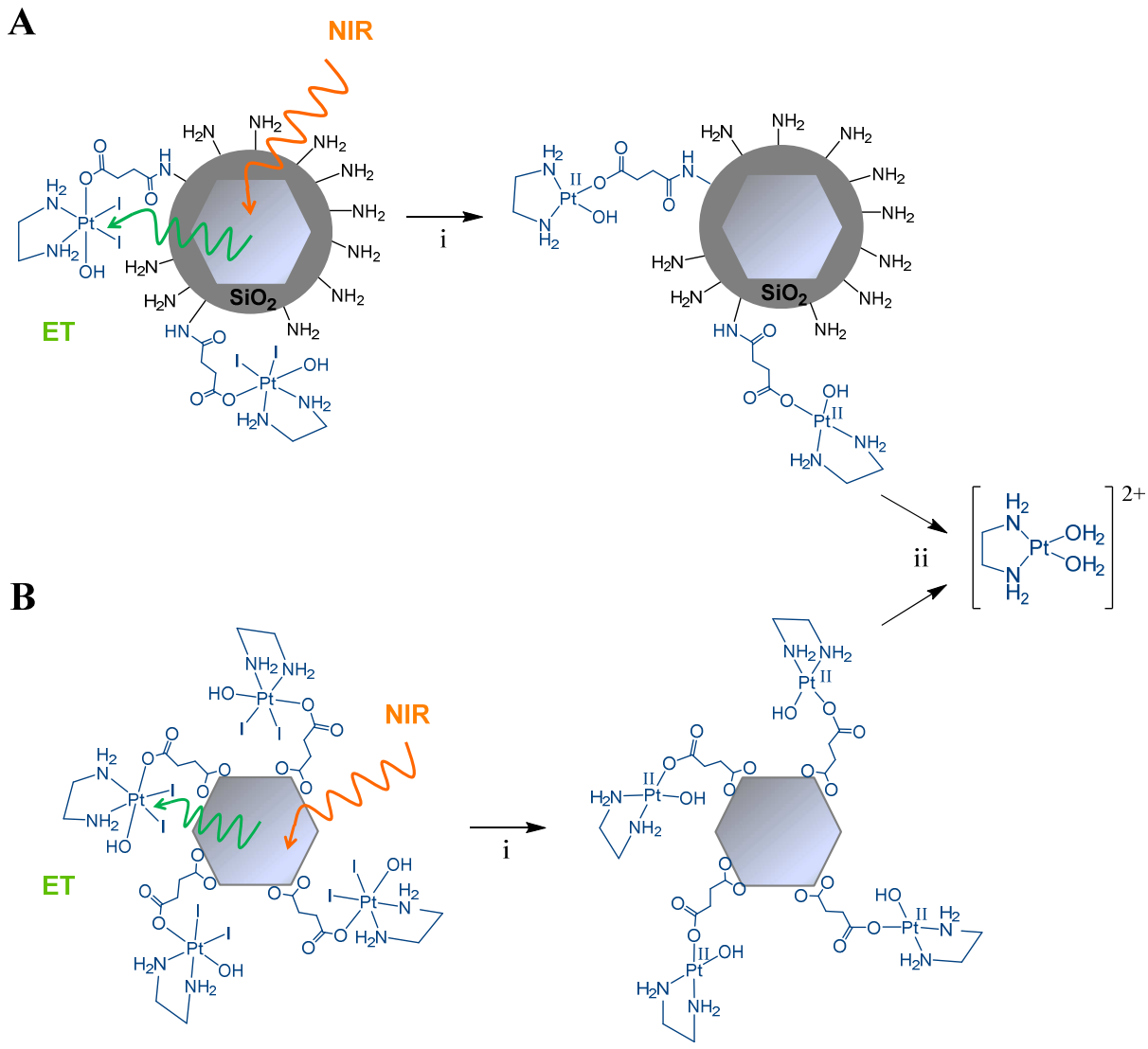

Figure 1. Strategies for attaching Pt(IV) antitumor prodrugs to UCNPs and the proposed mechanism of photoactivation by near infrared (NIR) radiation. **A**: Coupling by amide bond formation (*covalent conjugate*), **B**: Coupling by carboxylate exchange of oleate (*carboxylate construct*). The coupling of $NaGdF_4$:Yb,Er-UCNPs with complex **3** is shown as an example: i) Energy transfer (ET) of emitted light from UCNPs causes the reduction of Pt(IV) to Pt(II) with

loss of both iodido ligands, ii) aquation of the labile Pt(II) intermediate (i.e., substitution of carboxylato ligand for H_2O) with formation of the cytotoxic $[Pten(H_2O)_2]^{2+}$ species.

Experimental section

Materials and methods. K_2PtCl_4 and glutaric anhydride were purchased from Alfa Aesar (Karlsruhe, Germany). Succinic anhydride was obtained from Fluka Chemika (Neu-Ulm, Germany), pentanoic anhydride from Merck Schuchardt OHG (Hohenbrunn, Germany) and calf thymus DNA from Sigma-Aldrich (Steinheim, Germany). Anhydrous dimethylformamide (DMF) was from Merck, EMD Millipore (Darmstadt, Germany) and dimethyl sulfoxide (DMSO) from Roth (Karlsruhe, Germany). Rare earth oxides (99.9 %) were purchased from Alfa Aesar (Karlsruhe, Germany), oleic acid (tech. grade 90 %), 1-octadecene (tech. grade 90 %), trifluoroacetic acid (99 %) and sodium trifluoroacetate (98 %) from Sigma-Aldrich. 3-(ethyliminomethyleneamino)-*N*,*N*-dimethylpropan-1-amine (EDC) was from Acros organics (New Jersey, USA) and 1-hydroxy-2,5-pyrrolidinedione (NHS) was from Novabiochem (Läufelingen, Switzerland). The starting Pt(IV) complex *cis,trans*-$[PtI_2(OH)_2(en)]$ (**1**) was synthesized starting from K_2PtCl_4 as described elsewhere.[21] Water was purified by a Milli-Q-biocel system (Merck Millipore, Darmstadt, Germany).

Attenuated total reflection-Fourier transform infrared spectroscopy (ATR-FTIR) spectra were recorded with a Nicolet IR-200 FT-IR from Thermo Scientific. NMR spectra were recorded with a Bruker Ultrashield 400 (Rheinstetten) at 400.2 (^{1}H), 100.6 (^{13}C) and 86.0 (^{195}Pt) MHz in DMSO-d_6 at 298 K. ^{195}Pt chemical shifts were referenced relative to external K_2PtCl_6. UV/vis spectra were recorded with a Spekol 1200 diode array spectrophotometer from Analytik Jena GmbH (Jena, Germany) and Lamda 900 (Perkin Elmer, Rodgau, Germany). Flameless atomic

absorption spectrometric (AAS) measurements were made with a Unicam 989QZ AA spectrometer (Cambridge, UK) at λ = 265.9 nm with deuterium compensation. Thermogravimetric analysis (TGA) and differential scanning calorimetry (DSC) were carried out in a controlled atmosphere using the SDT 2960 Simultaneous DSC-TGA of TA Instruments. Thermograms were recorded at 10 °C min^{-1} heating rates in nitrogen flow. The covered temperature ranged from RT to 700 °C.

NIR light source. The NIR-laser used for the irradiation studies characterizing the stability of diiodido-Pt(IV) complexes, ct-DNA platination, Pt release from UCNPs and cytotoxicity was an infrared point laser module DH980-120-3(22×65) from Picotronic (Koblenz, Germany), which emits light of λ = 980 nm wavelength with an optical output power of 120 mW and a power density for light leaving the laser of 1.2 W/cm^2.

Synthesis of *trans,cis*-bis(3-carboxypropanoato)ethylenediaminediiodidoplatinum(IV) (2). A suspension of 73 mg (0.13 mmol) of *cis,trans*-[$PtI_2(OH)_2$(en)] (**1**)[16] in 4 mL of anhydrous DMF was allowed to react with 108 mg (1.1 mmol, 8 mol equiv.) of succinic anhydride for 5 h at 70 °C with constant stirring. The volume of the resulting red–brown solution was reduced until a brown oily residue remained. THF (5 mL) was added, and the solution briefly mixed. Pentane was added to precipitate the product. The isolated solid was purified by suspending in chloroform. The dark yellow product was filtered and dried under vacuum. Yield: 11 mg (11 %). ^{1}H NMR (DMSO-d_6): δ = 12.07 (s, 2H, OH), 8.24 (br s, 4H, NH_2), 2.49 (m, 12H, (en), H-3/H-4) ppm. ^{195}Pt NMR: δ = −325 ppm. IR: $\tilde{\upsilon}$ = 3160 (w, $\nu_{NH\text{-}as}$), 2996 (w, $\nu_{NH\text{-}symm}$), 2647 (w, ν_{CH}) and 1724 (m, ν_{CO}) cm^{-1}. UV/vis: λ_{max} = 385 nm (ε = 857 L · mol^{-1} · cm^{-1} in PIPES/$NaClO_4$ buffer

(pH 6.9)). ESI-HRMS: m/z 741.8728 pred., 741.8696 found for $[C_{12}H_{21}I_2N_2O_8Pt]^-$; m/z 809.8745 pred., 809.8725 found for $[C_{12}H_{22}I_2N_2O_8Pt + K]^+$.

Synthesis of *trans,cis*-(3-carboxypropanoato)ethylenediaminehydroxidodiiodido-platinum(IV) (3). A suspension of 45 mg (0.08 mmol) *cis,trans*-$[PtI_2(OH)_2(en)]$ (**1**) was allowed to react with 32 mg (0.32 mmol, 4 mol equiv.) succinic anhydride for 20 h at 65 °C with constant stirring. The resulted deep red solution was filtered and the solvent removed under reduced pressure. The orange-brown residue was suspended in ca. 1 mL acetone. This led to precipitation of a yellow solid, which increased by cooling for several hours at 0 °C. The isolated product was thoroughly washed with acetone. Yield: 30 mg (58%). ^{1}H NMR (DMSO-d_6): δ = 12.07 (s, 1H, C6-OH), 8.25 (br s, 2H, NH_2), 6.89 (br s, 2H, NH_2), 2.37–2.34 (m, 8H, H-1/H-2/H-4/H-5) ppm. ^{13}C NMR: δ = 181.6 (C3), 173.9 (C6), 49.0 (C1/2), 31.7 (C4), 30.0 (C5) ppm. ^{195}Pt: δ = −334 ppm. IR: $\tilde{\upsilon}$ = 3428 (w, ν_{OH}), 3153 (w, $\nu_{NH\text{-}as}$), 3055 (w, $\nu_{NH\text{-}symm}$), 2947 (w, $\nu_{CH\text{-}as}$), 2847 (w, $\nu_{CH\text{-}symm}$), 1704 and 1660 (m, ν_{CO}), 1560 (m, δ_{CH}) cm^{-1}. UV/vis: λ_{max} = 379 nm (ε = 1750 $L \cdot mol^{-1} \cdot cm^{-1}$ in H_2O). ESI-MS: m/z 642.1 pred., 641.7 found for $[C_6H_{13}I_2N_2O_5Pt]^-$; m/z 666.0 pred., 664.9 found for $[C_6H_{14}I_2N_2O_5Pt + Na]^+$.

Synthesis of *trans,cis*-(4-carboxybutanoato)ethylenediaminehydroxidodiiodido-platinum(IV) (4). In a flamed-dried flask were added 58 mg (0.11 mmol) *cis,trans*-$[PtI_2(OH)_2(en)]$ (**1**) and 54 mg (0.47 mmol, 4 mol equiv.) glutaric anhydride followed by 3.5 mL of anhydrous DMF. The reaction mixture was stirred at 65 °C for 24 h to give an orange-colored solution which was evaporated to dryness. To obtain the product, the orange-brown residue was suspended in 3 mL of acetone. The yellow precipitate was allowed to cool on ice for several

hours, was filtered under suction and washed thoroughly with acetone. Yield: 28 mg (39%). ^{1}H NMR: δ = 11.93 (br s, 1H, C7-OH), 8.34 (br s, 2H, NH_2), 6.88 (br s, 2H, NH_2), 2.36–2.32 (m, 4H, H-1/H-2), 2.24–2.20 (m, 2H, H-6), 2.14–2.09 (m, 2H, H-4), 1.65–1.62 (m, 2H, H-5) ppm. ^{13}C: δ = 182.4 (C3), 174.4 (C7), 49.0 (C1/2), 36.0 (C4), 33.0 (C6), 21.0 (C5) ppm. ^{195}Pt: δ = −332 ppm. IR: $\tilde{\upsilon}$ = 3130 (w, ν_{NH}), 2952 (w, ν_{NH}), 2915 (s, $\nu_{CH\text{-}as}$), 2847 (m, $\nu_{CH\text{-}symm}$), 1699 (w, ν_{CO}), 1660 (m, ν_{CO}), 1571 (m, δ_{CH}), 720 (CH_2-rocking) cm^{-1}. UV/vis: λ_{max} = 373 nm (ε = 2113 L · mol^{-1} · cm^{-1} in phosphate buffer, pH 7.4). ESI-MS: m/z 656.09 pred., 656.00 found for $[C_7H_{15}N_2O_5I_2Pt]^-$; 679.87 pred., 679.75 found for $[C_7H_{16}N_2O_5I_2Pt + Na]^+$.

Synthesis of oleate-capped β-$NaGdF_4$:Yb(20%),Er(2%) and β-$NaGdF_4$:Yb(20%),Tm(0.5%). Oleate-capped UCNPs were prepared via thermal decomposition procedure previously reported.[22] Briefly, all the rare earth trifluoroacetate precursors were synthesized by mixing 353.4 mg (1.95 mmol) Gd_2O_3, 98.5 mg (0.5 mmol) Yb_2O_3 and 9.6 mg (0.05 mmol) Er_2O_3 for the Er doped UCNPs and 360.7 mg (1.99 mmol) Gd_2O_3, 98.5 mg (0.5 mmol) Yb_2O_3 and 2.4 mg (0.0125 mmol) Tm_2O_3 for the Tm doped UCNPs with 5 mL distilled H_2O and 5 mL trifluoroacetic acid in a three-neck round-bottom flask. The reaction mixture was stirred under reflux at 80 °C until a clear solution was obtained after which the solvent was allowed to evaporate at 60 °C on a water-bath without stirring. In the second step 340.5 mg (2.5 mmol) sodium trifluoroacetate was added to the dried lanthanide trifluoroacetate precursors along with 7.5 mL of 1-octadecene and 7.5 mL of oleic acid (solution A). In a separate three-neck round bottom flask 12.5 mL of the coordinating oleic acid and 12.5 mL of the non-coordinating solvent 1-octadecene were added (solution B). Both solutions were heated to 125 °C under vacuum with magnetic stirring to remove residual water and oxygen. Successively, the

solution B (reaction vessel) was placed under Ar gas and the temperature was increased to 310 °C and the solution A was added to the reaction vessel by means of a syringe and pump system at a rate of 1.5 mL/min. The solution was maintained at this temperature and stirred vigorously for 1 h. The mixture was allowed to cool to RT, the UCNPs were precipitated by the addition of hexane/ethanol (1:4 v/v) and isolated via centrifugation at 4000 RPM for 15 minutes. The resulting pellet was then washed once with ethanol and further purified by dispersing in a minimum amount of hexane and precipitated with excess ethanol. Following centrifugation, the resulting pellet was stored in 2 mL of ethanol. A small amount of powder was dried under vacuum for XRD characterization.

Preparation of amino-modified UCNPs. The surface functionalization was carried out according to modified approaches reported in the literature.[23, 24] Twenty milligrams of oleate-capped UCNPs were dispersed in 50 mL 2-propanol by sonication and agitation for 30 min. Twenty milliliters of water and 3 mL of an ammonia solution were added. After vigorously stirring the mixture at 40 °C for 20 min, 50 µL (0.23 mmol) tetraethoxysilane (TEOS) in 20 mL of 2-propanol were added dropwise within 30 min. After incubation at RT for 4 h, a solution containing (3-aminopropyl)triethoxysilane (APTES) (600 µL, 2.6 mmol) in 2-propanol (25 mL) was added dropwise into the mixture within 30 min. After 18 h incubation, the precipitate was collected by centrifugation (8000 RPM, 10 min), washed four times with ethanol by sonication and dried under vacuum to yield UCNPs with an aminated silica-shell. Figure S1 shows the FTIR spectrum of the isolated powder.

Conjugation of amino-modified UCNPs with diiodido-Pt(IV) complexes 3 and 4. The synthesis of conjugates of the type $NaGdF_4$:Yb,Er-SiO_2-NH-**Pt** was carried out by using standard amide coupling reaction.[25] Six milligrams (31 μmol) 3-(ethyliminomethyleneamino)-*N*,*N*-dimethylpropan-1-amine (EDC) and 4 mg (35 μmol) 1-hydroxy-2,5-pyrrolidinedione (NHS) were dissolved in 10 mM 1,4-piperazinediethanesulfonic acid (PIPES)/$NaClO_4$ buffer of pH 6.9 (0.5 mL) and left at RT for 10 min. To this solution were added 0.1 mol equiv. Pt complex **3** or **4** (~2 mg, 3.1 μmol). The mixture was allowed to stand at RT for 10 min protected from light. Afterwards, the mixture was added to a dispersion consisting of 8 mg UCNPs in 1 mL of 10 mM piperazine-*N,N′*-bis(2-ethanesulfonic acid) (PIPES)/$NaClO_4$ buffer (pH 6.9). The reaction mixture was sonicated for 2 min and then shook for 48 h at 37 °C in a water bath. The resulting pale yellow conjugates $NaGdF_4$:Yb,Er-SiO_2-NH-**3** or $NaGdF_4$:Yb,Er-SiO_2-NH-**4** were isolated by centrifugation (10000 rpm, 10 min), thoroughly washed with 1 mL10 mM PIPES/$NaClO_4$ buffer (pH 6.9), 1 mL water and with 1 mL ethanol (twice) and dried under vacuum. The amount of Pt bound to the conjugates $NaGdF_4$:Yb,Er-SiO_2-NH-**3** and $NaGdF_4$:Yb,Er-SiO_2-NH-**4**, was measured by flameless atom absorption spectroscopy (AAS) and found to be 1.88 and 1.32 μg Pt/mg UCNP, respectively.

Attachment of Pt(IV) complexes to UCNPs by exchange with oleate. Twenty eight milligrams of oleate-capped UCNPs were dispersed in a solution consisting of 7 mg (11 μmol) of Pt(IV) complex **3** or **4** in 2 mL of 10 mM PIPES/$NaClO_4$ buffer (pH 6.9) by sonification (ratio Pt/oleate 1.1). The ratio was estimated by differential scanning calorimetry-thermal gravimetric analysis (DSC-TGA) in respect to the nanoparticles with 10 % oleate. The reaction mixture was allowed to shake at RT while kept in the dark for 3 d. During this time the formation of an oleic

acid phase was observed, indicating displacement of oleate by the Pt(IV) complexes. The nanoparticles were occasionally sonicated. The resulting pale yellow constructs $NaGdF_4$:Yb,Er(or Tm)-**3/4** were collected by centrifugation (9000 RPM, 10 min), washed twice with PIPES/$NaClO_4$ buffer (pH 6.9), once with 2-fold deionized water and ethanol, and were dried under vacuum. A near quantitative displacement of oleate for Pt(IV) appeared to have been achieved, as evidenced by the absence of bands ascribable to oleate in the FTIR spectrum of the construct (Figure S2). The amount of Pt bound to the constructs $NaGdF_4$:Yb,Er-**3** and $NaGdF_4$:Yb,Er-**4**, was measured by AAS and found to be 1.21 and 1.00 μg Pt/mg UCNP, respectively.

Measurement of Pt content of modified UCNPs. Samples of Pt modified UCNPs were accurately weighed and suspended in 0.5% HNO_3 solution at concentrations between 1.00 – 1.50 mg UCNP/mL. The samples were sonicated with warming for ca. 15 min before being analyzed by AAS by using the temperature program shown in Table S1. Calibration was done with nine external Pt standards between 100 and 500 ppb by peak area for quantification. Each standard and sample was measured in triplicate and averaged.

X-ray photoelectron spectra (XPS). XPS were recorded by using a Perkin-Elmer PHI 5600 ci spectrometer with a standard Al-Kα source (1486.6 eV) working at 250 W. The working pressure was less than 7×10^{-7} Pa. The spectrometer was calibrated by assuming the binding energy (BE) of the Au $4f_{7/2}$ line to be 84.0 eV with respect to the Fermi level. Extended spectra (survey) were collected in the range 0–1350 eV (187.85 eV pass energy, 0.5 eV step, 0.025 s · $step^{-1}$). Detailed spectra were recorded for the following regions: Pt 4f, I 3d, N 1s, O 1s, Si 2p,

Na 1s and C 1s (23.5 eV pass energy, 0.1 eV step, 0.2 s · $step^{-1}$). The reported binding energy (BEs, standard deviation = ± 0.1 eV) were corrected for the charging effects by considering the adventitious C 1s line at 285.0 eV. The atomic percentage, after a Shirley type background subtraction[26], was evaluated by using the PHI sensitivity factors.[27] Samples for the XPS analysis were evacuated for 12 h at ca. 1×10^{-3} Pa before measurements.

Transmission electron microscopy (TEM). The size and morphology of UCNPs were observed with a Tecnai G2 (FEI) transmission electron microscope operating at 100 kV. Images were captured with a Veleta (Olympus Soft Imaging System) digital camera. Samples were drop cast on carbon-coated grids (400 mesh Cu).

X-ray diffraction (XRD). X-ray diffraction measurements were carried out with a Bruker D8 Advance diffractometer using Cu Kα radiation (λ = 1.5406 Å).

Emission spectra. Upconversion emission spectra of UCNPs were performed on Fluorolog-3 (Horiba Jobin Yvon) spectrofluorimeter by using an external 0–2 W adjustable λ = 980 nm CW laser diode (CNI) as excitation source.

Photodecompositon studies. The ability of UCNPs to degrade Pt(IV) complexes when irradiated with a NIR laser (λ = 980 nm) were monitored by UV/vis spectroscopy. In a solution of Pt complex (500 μM) in 10 mM PIPES/$NaClO_4$ buffer (pH 6.9), the UCNPs were dispersed at 3 mg/mL. The dispersion was irradiated in a cuvette with continuous stirring for 3.5 h with the laser. At specified time intervals, UV-vis spectra were recorded. For controls, a solution of Pt

complex without UCNPs was irradiated with the laser while another solution of Pt complex with UCNPs was kept in the dark.

Measurement of Pt release from modified UCNPs. Flameless AAS was used in the Pt release experiments. Therefore, the conjugate or construct (0.5 mg/mL) was dispersed in 10 mM PIPES/$NaClO_4$ buffer (pH 6.9) and one part of the resulting colloidal solution was irradiated in a cuvette from the top with the NIR laser under stirring. Controls without irradiation were performed with the other fraction of dispersion. After defined periods of time a 100 µL-aliquot was taken and centrifuged. 80 µL of the supernatant was separated and frozen at −20 °C. The last sample was taken after 5 h of irradiation with the NIR laser and subsequent incubation for 19 h in the dark at RT. On the day of AAS analysis the aliquots were centrifuged again and 70 µL of the sample were diluted in PIPES/$NaClO_4$ buffer (pH 6.9). The amount of Pt released was quantified by AAS using the temperature-time program in Table S1. Calibration was done with 4-7 external Pt standards between 30 and 650 ppb by using peak height for quantification. Each standard and sample was measured in triplicate and averaged.

Measurement of Pt binding to ct-DNA. The method used was a modification of those previously published.[21, 28] A 20 mM stock solution of Pt complex in DMF was 1000-fold diluted in a dispersion of $NaGdF_4$:Yb,Er-UCNPs (0.8 mg/mL) in 10 mM PIPES/$NaClO_4$ buffer (pH 6.9) and irradiated from the top in a cuvette with NIR-laser under stirring while an identical solution was kept in the dark. After 4 h of irradiation the UCNPs were removed by centrifugation and the supernatant was added to an equal volume of 0.50 mg/mL ct-DNA in 10 mM PIPES/$NaClO_4$ buffer (pH 6.9) (finally DNA concentration 0.25 mg/mL). The mixture was incubated by shaking

at 37 °C in the dark. At various time intervals 300 µL-aliquots were taken and mixed with 150 µL ice-cold 0.9 M Na-acetate. The DNA was precipitated with 930 µL ice-cold ethanol. The samples were frozen in liquid nitrogen and stored at −20 °C till all samples were taken. The precipitates were separated by centrifugation at −9 °C (5400 g, 10 min). After removal of the supernatant, the DNA pellet was taken up in 300 µL 0.3 M Na-acetate. The precipitation was caused by the addition of 900 µL ice-cold ethanol. The samples were thawed at −20 °C for at least 30 min. The DNA was collected by centrifugation, washed three times with 600 µL ethanol and hydrolyzed in 500 µL 0.5 % HNO_3 at 70 °C for 48 h. The Pt content in these ct-DNA samples was determined by flameless AAS by using the temperature-time program according to Table S1. Calibration was done with 4-7 external Pt standards between 30 and 650 ppb by measuring peak height for quantification. Each standard and sample was measured in triplicate and averaged. Afterwards, the amount of DNA in each sample was determined by UV/vis-spectrometry at 260 nm with $\varepsilon = 8900\ M^{-1} \cdot cm^{-1}$.

Cell culture. The adherent human cancer cell lines (SISO cervix cancer line, LCLC-103H large lung cancer line) as well as the leukemia cell line HL60 were obtained from the German Collection of Microorganisms and Cell Culture (DSMZ, Braunschweig, Germany) while the A2780 and A2780cis ovarian cancer lines were a gift of Dr. Julie Woods, University of Dundee, UK. Cells were grown in RPMI cell culture medium 1640 from PAN Biotech (Aidenbach, Germany) supplemented with 10 % fetal calf serum and antibiotics (penicillin and streptomycin), and kept at 37 °C in humidified atmosphere of 5 % CO_2. For the *in vitro* phototoxicity studies of diiodido-Pt(IV) complexes **3** and **4** UVA irradiation (λ_{max} = 352 nm) and white light were generated with Hitachi FL 8BL-B 8 W lamps and cool white fluorescent 8 W mercury tubes,

respectively. The experimental setup has been described elsewhere.[29, 30] Briefly, five lamps were fitted into a Luzchem Expo panel (Luzchem Research Inc., Ontario, Canada) and positioned 25 cm above the microtiter plates in the incubator. Lower wavelength radiation ($\lambda < 300$ nm) was blocked by an acrylic glass filter.

The crystal violet method was used for the estimation of antiproliferative activity of **3** and **4** in the adherent cell lines SISO, LCLC-103H, A2780 and A2780cis, as previously described in detail.[31] Cells were seeded in 100 µL medium at a density of 1000 cells per well (SISO, A2780) and 250 cells per well (LCLC-103H) and incubated for 24 h. Afterwards, the cells were treated with a series of five dilutions of Pt complexes (0.1 v/v% DMF). 100 µL of the working dilutions were added to each well. The plates were returned to the incubator. After preincubation for 1 h, the treated cells were irradiated with UVA or white light for 2 h. Subsequently the cells were incubated in the dark for 6 h before the medium was replaced by fresh culture medium. After an additional incubation for 87 h, the medium was discarded from the plates. Cells were fixed with glutaraldehyde solution (1 v/v %) and stained with crystal violet (0.02 %). The OD was measured at $\lambda = 570$ nm with a 2010 plate reader (Anthos) and IC_{50} values were estimated by linear least-squares regression of the growth values versus the logarithm of the substance concentration.

The cell experiments with UCNPs were carried on with HL60 human leukemia cell line and performed by using the NIR laser and culture medium without phenol red. Cytotoxicity was measured with a MTT method as described elsewhere.[31, 32] Briefly, after irradiation procedure of HL60 cells, the cells were seeded into 96-well microtiter plate and incubated for 48. A freshly prepared solution of MTT in PBS (20 µL at 2.5 mg/mL) was added to each well and the plate was returned to the incubator. Following a 4 h incubation, 100 µL/well of 0.04 N HCl in 2-

propanol was added and upon dissolution of the formazan the optical density was measured at λ = 570 nm.

Cytotoxicity of UCNP conjugates and constructs with NIR irradiation. The UCNP conjugates/constructs were dispersed at 0.2 mg/mL by sonification in culture medium without phenol red. Four milliliters of the dispersion were mixed with an equal volume of the HL60-cell-suspension (120000 cells/mL), then 4 mL of resulting mixture were incubated in a 25 cm^3-flask in the dark and the residual mixture was transferred in one well of a six-well-plate. The plate was placed in the incubator and the mixture was irradiated with the NIR-laser from the top accompanied by very gentle stirring with a magnetic stir bar. The total irradiation duration was 3 h with 15 min without NIR-light after 30 min of irradiation. A suspension (60000 cells/mL) was kept in the dark and served as a second control. After exposure to the NIR laser, cells were plated out in 96 well plates and incubated for 44 h. The cells were then stained with 3-(4,5-dimethylthiazol-2-yl)-2,5-diphenyltrazolium bromide (MTT). In a separate experiment, a cell suspension (60000 cells/mL) lacking UCNPs was irradiated in the same manner in order to evaluate the effect of the NIR-laser alone on cell growth.

Results

Synthesis and characterization of the diiodido-Pt(IV) complexes.

The reaction of K_2PtCl_4 with KI, followed by the addition of ethylene diamine and subsequent oxidation of the isolated [PtI_2(en)] with H_2O_2 led to the starting complex **1** bearing two hydroxido groups in axial position.[21] The esterification reaction with 8 mol equiv. succinic anhydride produced the symmetric complex **2** in low yield, whereas the reaction of **1** with just 4

mol equiv. anhydride gave the asymmetric monosuccinato-Pt(IV) complex **3** in moderate yield (Scheme 1). In analogous synthesis, the formation of ester **4** was achieved by using glutaric anhydride. ^{1}H-NMR confirmed the formation of the monocarboxylate Pt(IV) complexes **3** and **4**; both complexes showed two distinct broad singlets at ca. $\delta = 8.3$ and 6.9 ppm, which were assigned to the pairs of unsymmetrical NH_2, while the symmetrical dicarboxylato-Pt(IV) complex **2** showed only one broad singlet at ca. $\delta = 8.3$ ppm, which was assigned to the pair of symmetrical NH_2 groups. Moreover, a comparison of the intensities of the signals ascribable to methylene groups of complexes **3** (H-4/H-5) and **4** (H-4/H-5-/H-6), respectively, with the intensities of the singlets corresponding to the coordinating NH_2 groups, gave evidenced that acylation at only one of the two hydroxido ligands had occurred for **3** and **4**.

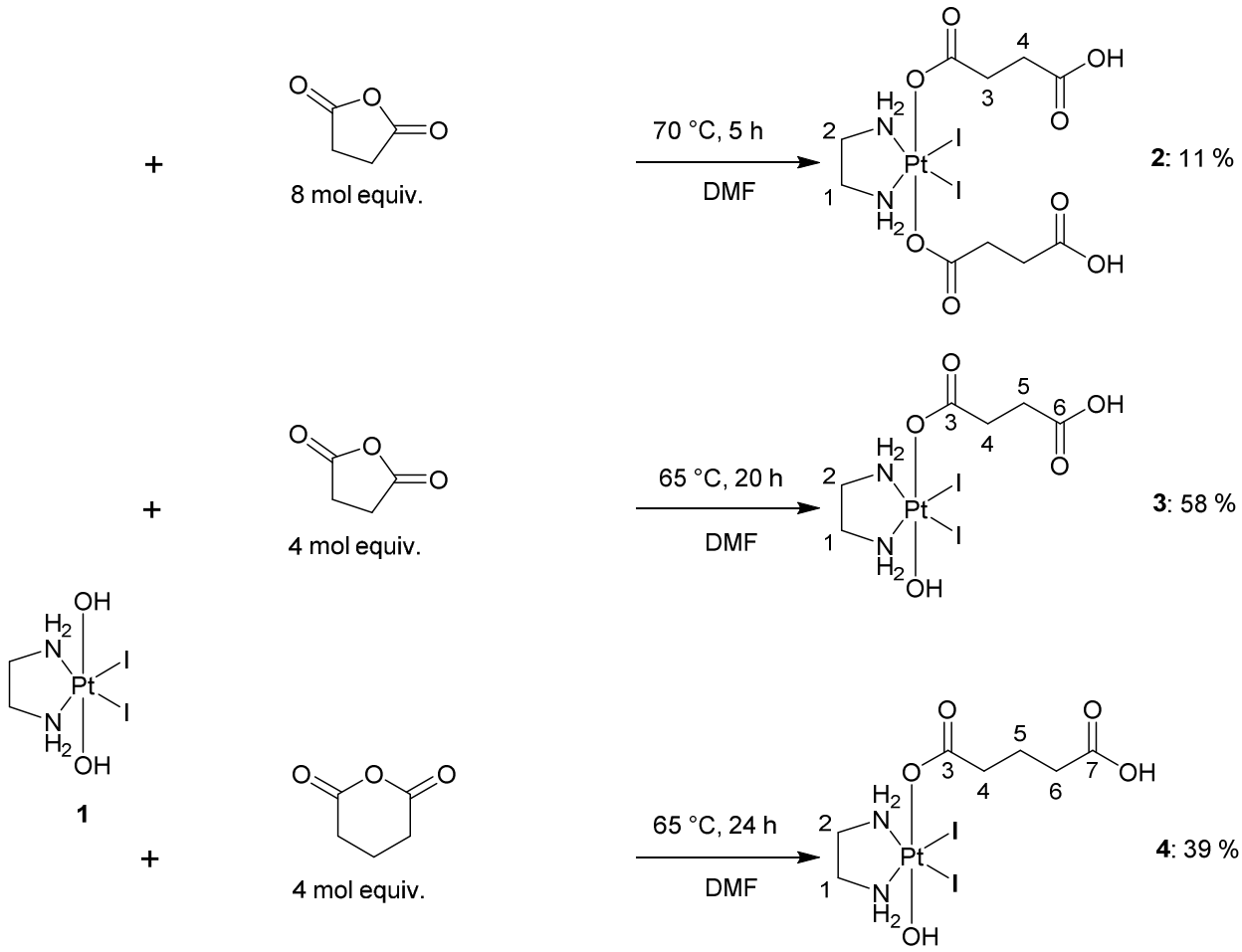

Scheme 1. Synthesis of carboxylated diiodido-Pt(IV) complexes.

Irradiation induced antiproliferative activity of Pt complexes. To confirm a mechanism of photoactivation, the effects of UVA (λ_{max} = 352 nm) or visible light on the cytotoxic activity of the synthesized diiodido-Pt(IV) complexes **3** and **4** were investigated with the human cancer cell lines SISO (human cervix cancer), LCLC-103H (human large cell lung cancer), A2780 (human ovarian cancer), and HL60 (human leukemia). (Complex **2** was not investigate for cytotoxicity because of the very small amounts of this compound available due to poor synthetic yields.) For these studies, dark controls were performed parallel to the irradiated samples. Irradiation of all four cell lines alone with UVA light for 2 h had no effect on cell growth (data not shown). The growth of cells treated with either complexes **3** or **4** resulted in decreases in the IC_{50} values, in some cases by significant amounts (*$p < 0.05$), when the incubations were irradiated in combination with UVA for 2 h compared to the dark controls. For example, UVA caused a 20 % significant increase in potency of complex **3** in A2780 cell line compared to dark controls. In the SISO line, **4** showed a 23 % significant increase in cell growth inhibition potency when co-irradiated with UVA, while the IC_{50} value of **4** against LCLC-103H also decreased significantly by 40 % after irradiation (Table 1). The cisplatin resistant cell line A2780cis was cross-resistant to both **3** and **4**; interestingly, irradiation with UVA of **4** in the A2780 versus A2780cis cell lines resulted in the same level of resistance (RF = 2.38) compared to without irradiation (RF = 2.34), suggesting that a similar cytotoxic species forms both in the dark as well as during photoactivation. With the suspension cell line HL60, **3** showed a 48 % increase of cell growth inhibition when co-irradiated with UVA light whereas no change in the potency was observed with **4**. (Table 1)

Table 1. Calculated IC_{50} values (μM, means ± standard deviation) for **3** and **4** in five human cancer cell lines, without and with irradiation with UVA (λ_{max} = 350 nm, I = 0.12 mW/cm^2) for 2 h at 37 °C (n = 3 independent experiments; significance determined by two-sided, paired t-test: *p < 0.05).

	SISO		LCLC-103H		A2780		A2780cis		HL60	
	dark	UVA	dark	UVA	dark	UVA	dark	UVA	dark	UVA
3	7.08 ± 2.50	5.72 ± 1.44	> 80	40.66 ± 7.61	20.95 ± 2.34*	16.70 ± 1.79*	> 40	> 40	51.36 ± 3.47*	26.51 ± 6.65*
4	8.09 ± 4.55*	6.14 ± 4.19*	60.33 ± 13.00 *	37.09 ± 7.91*	12.03 ± 1.78	9.22 ± 1.33	28.17 ± 5.16 RF = 2.34	21.91 ± 5.57 RF = 2.38	47.53#	51.82#

RF = resistance factor, #: n = 2

The cytotoxic potency of **4** in the SISO cell line also increased significantly by 36% when white light was used as an irradiation source compared to dark controls (Table 2). In all other cases, IC_{50} values decreased when white light was combined with treatment of **3** and **4** but the differences were not statistically significant (Table 2). Surprisingly, we found that white light has a selective cytotoxic effect on the growth of the cisplatin resistant A2780 line, A2780cis, thus this cell line was left out of these studies. In conclusion, the majority of these studies indicate that both UVA and white light can photoactivate the diiodido-Pt(IV) diamines to cytotoxic species.

Table 2. Calculated IC_{50} values (µmole/L, means ± standard deviation) for **3** and **4** in adherent cancer cell lines, without and with irradiation with white light (I = 0.65 mW/cm^2) for 2 h at 37 °C (n = 3–4 independent experiments; significance determined by two-sided, paired t-test: *p < 0.05).

	SISO		LCLC-103H		A2780	
	dark	white light	dark	white light	dark	white light
3	10.79 ± 4.02	7.01 ± 1.21	> 40	19.34 ± 8.85	20.86 ± 9.31	10.60 ± 2.57
4	10.50 ± 3.69*	6.74 ± 2.44*	> 40	25.34 ± 15.38	13.20 ± 3.55	8.07 ± 1.78

Preparation and properties of UCNPs. $NaGdF_4$:Yb,Er(or Tm) upconverting nanoparticles were synthesized by using high-temperature colloidal methods, which result in UCNPs coated with oleate ligands. XRD patterns of oleate-capped $NaGdF_4$:Yb,Er(or Tm) nanoparticles are shown in Figure 2 A. All of the diffraction peaks can be indexed to β-$NaGdF_4$ with hexagonal phase and are in good agreement with the XRD pattern of standard $NaGdF_4$ [JCPDS# 27-0699]. Characteristic upconversion emission spectra of the oleate-capped $NaGdF_4$:Yb,Er(or Tm) upon 980 nm cw laser excitation are shown in Figure 2B. In the inset of Figure 2B a digital photograph of both Yb,Tm-doped and Yb,Er-doped UCNPs dispersed in toluene under 980 nm laser excitation is shown. TEM images of the prepared oleate-capped Er-doped UCNPs (Figure 3A-D) gave evidence of single crystalline nearly monodispersed hexagonal nanoparticles with a diameter of 48.5 ± 1.2 nm and a thickness of 22 nm (for oleate-capped Tm-doped UCNPs see Figure S3 in SI).

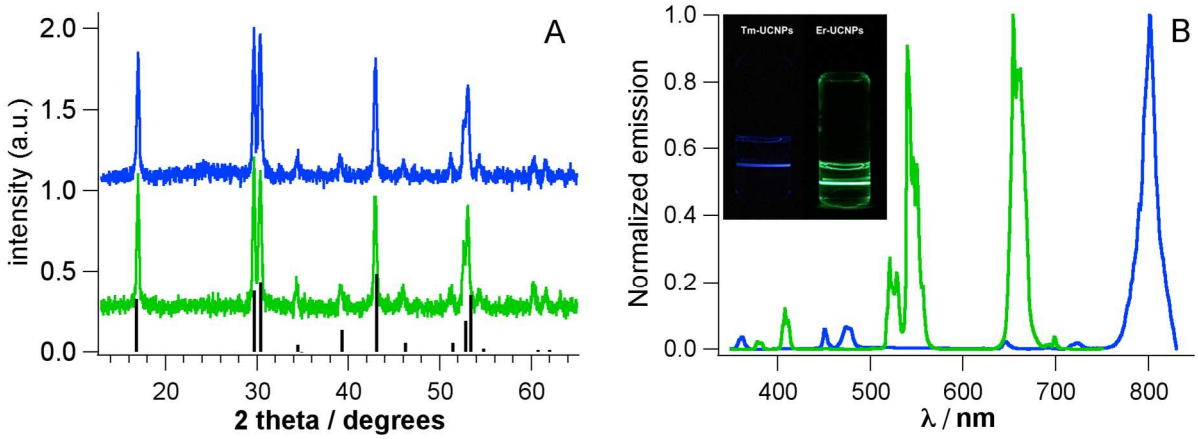

Figure 2. A: XRD patterns of oleate-capped $NaGdF_4$:Yb,Tm (blue line) and $NaGdF_4$:Yb,Er (green line). Standard reference pattern of β-$NaGdF_4$ (JCPDS# 27-0699) is also showed. B: Upconversion emission spectra and digital photograph of the upconversion luminescence in 0.1 wt% colloidal dispersion of nanoparticles in toluene, excited with NIR light (λ = 980 nm): $NaGdF_4$:Yb,Tm (blue line) and $NaGdF_4$:Yb,Er (green line).

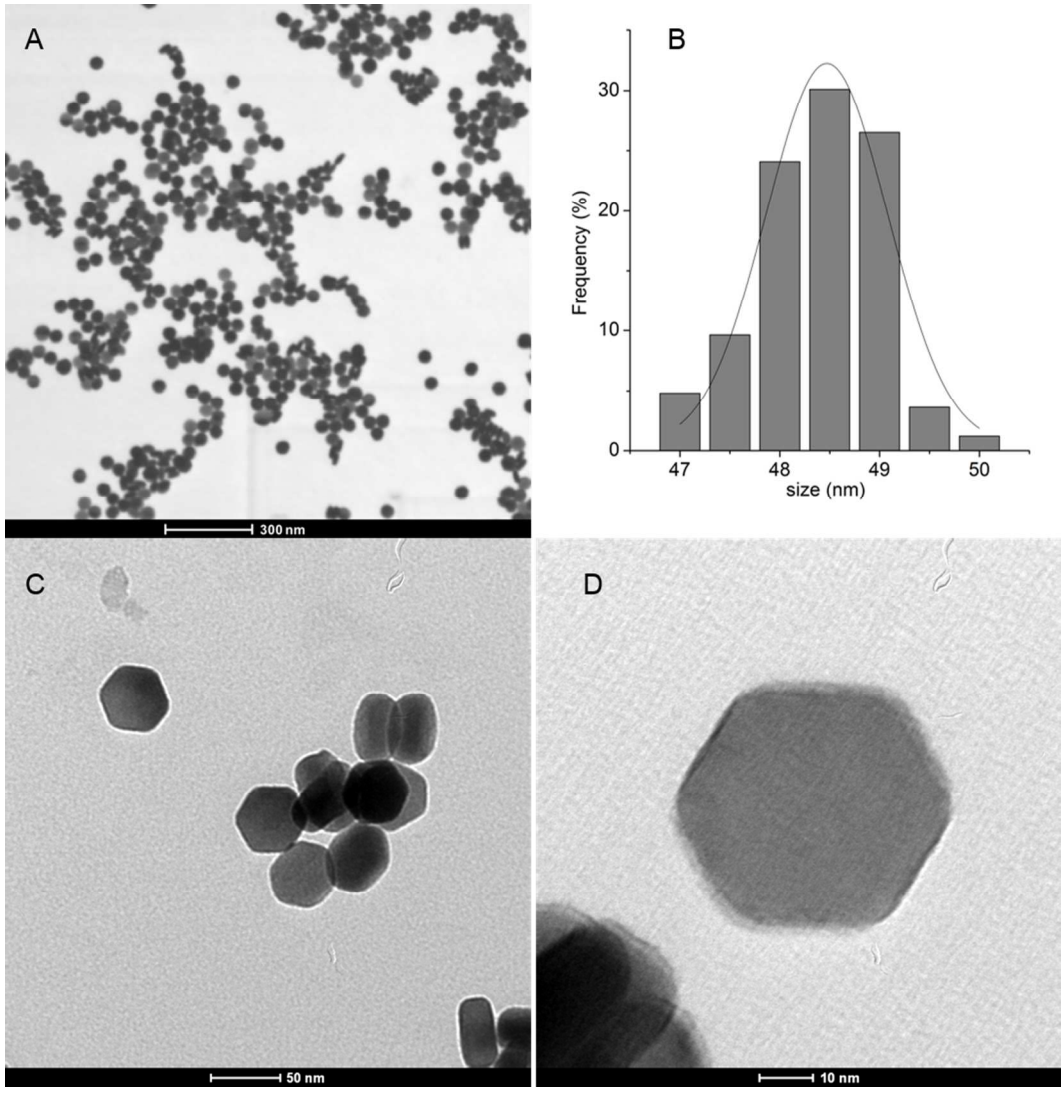

Figure 3.TEM images at different magnifications (A, C, D) and size distribution (B) of oleate-capped $NaGdF_4$:Yb,Er nanoparticles.

In order to covalently attach Pt complexes via their free carboxylate groups, the prepared oleate-capped UCNPs doped with Er were coated with a silica shell layer functionalized with amino groups. By using the Stöber process, the UCNPs were embedded in amorphous silica and

then aminated by basic hydrolysis of the amino-terminated silane coupling agent APTES. The success of the functionalization was confirmed by FTIR characterization. As shown in Figure S1 the spectrum of as prepared oleate-capped UCNPs exhibits transmission bands at 1554 and 1464 cm^{-1} corresponding to the asymmetric and symmetric stretching vibrations of carboxylate groups, respectively. Moreover, the two bands at 2926 and 2852 cm^{-1} can be assigned to the antisymmetric and symmetric stretching vibrations of the methylene groups, respectively, which are present in the long alkyl chain of the oleic acid molecule. The main band in the silicate-modified UCNPs is the strong transmission associated with the symmetrical stretching vibration of the Si−O bond at 1008 cm^{-1}.[33] This band is also present in the amino-modified UCNPs (Figure S1). Moreover in the amino-modified UCNPs two bands at 2930 and 2877 cm^{-1}, ascribable to the antisymmetric and symmetric stretching vibrations of methylene groups, respectively, coming from the new aminopropyl group, are evident. Hence, these results confirm the successful preparation of amino-modified UCNPs.

Further information on surface composition was obtained by XPS analysis. The peak positions observed for Si 2p, O 1s and N 1s core level (Table S2) are in agreement with those reported in literature for silicon and oxygen in silica, and nitrogen in amine groups, respectively.[33] Moreover Si, O and N are the only species observed on the surface suggesting that UCNPs are well capped. XPS quantitative analysis allowed to estimate that the amount of nitrogen on the nanoparticles surface was around 15 % (Table S3).

Figure S4 shows the results of TEM analysis of $NaGdF_4$:Yb,Er-SiO_2-NH_2 UCNPs. The thickness of silica shell surrounding the UCNPs is ca. 75 nm. In most of the cases more UCNPs are enclosed in a common silica shell, while relatively few appear as single spherical structures. While this clustering will reduce the surface area of the UCNPs and hence their loading

efficiency of Pt, it seems unlikely that such clustering will influence the activation process of the covalent conjugates.

Photochemistry studies of diiodido-Pt(IV) diamines with UCNPs. For successful energy transfer the absorption band of the light-sensitive Pt(IV) complex must overlap with at least one emission band of the nanoparticles. As shown in Figure 4 the LMCT bands of complex **2** (λ_{max} = 385 nm), complex **3** (λ_{max} = 379 nm) and complex **4** (λ_{max} = 373 nm) overlaps with the emission bands at λ = 345 nm, 358 nm, 450 nm and 476 nm in the case of Yb,Tm-doped UCNPs and at λ = 380 and 408 nm in the case of Yb,Er-doped UCNPs. Thus, these UCNPs would appear to be applicable for activating diiodido-Pt(IV) diamines with NIR.

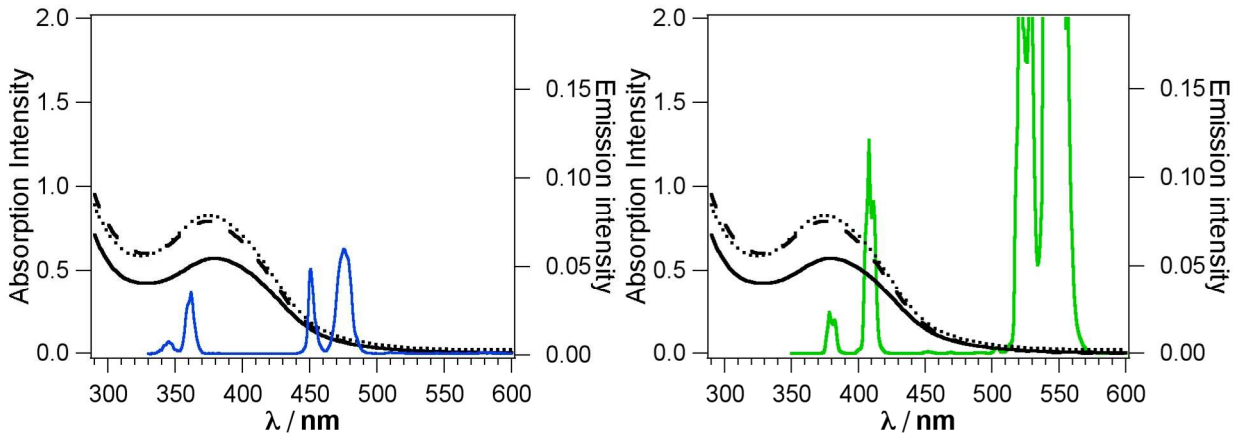

Figure 4. Absorption spectra of complex **2** (black continuous line), complex **3** (black dottted line) and complex **4** (black dashed line) in water and emission spectra of oleate- capped $NaGdF_4$: Yb,Tm (blue line) and oleate-capped $NaGdF_4$: Yb, Er (green line) in toluene.

Before attaching the Pt(IV) complexes to UCNPs, we investigated whether UCNPs could facilitate a photodecomposition of diiodido-Pt(IV) ethylenediamines by NIR in solution (i.e., if NIR together with UCNPs causes the diiodio-Pt(IV) prodrug to undergo photochemical reactions that lead to the loss of the LMCT band). For these studies, UV/vis-spectroscopy was used to measure decreases in the LMCT bands of the Pt complexes when mixtures of UCNPs and Pt(IV) complexes were irradiated with the NIR-laser (120 mW, λ = 980 nm). Representative for the diiodido-Pt(IV) complexes we present the UV/vis-spectra changes of the disuccinato Pt(IV) complexe **2** in 10 mM PIPES/$NaClO_4$ buffer (pH 6.9) during irradiation with NIR (Figure 5). Solutions of **2** are stable in the dark (Figure 5 B) and relatively stable when irradiated with the NIR laser (Figure 5A), while when they are irradiated with NIR laser in presence of UCNPs, the LMCT bands (I $\rightarrow$ Pt) at λ = 385 nm decreased in intensity over 3.5 h (Figure 5C and 5D). A subsequent incubation in the dark for 24 h led to a further decrease in the absorption band but no bands indicative of a decomposition product appeared. While the Tm-doped UCNP appeared to lead to a more rapid photodecomposition compared to the Er-doped nanoparticles. (Figure 5C and D), we chose to do use the Er-UCNPs for most of our studies because the emission spectra of these UCNPs appeared more advantageous compared to the Tm-UCNPs; the Tm-UCNPs have their strongest emission at ca. 800 nm (Figure 2B), which is not at all useful for photoactivation of diiodio-Pt(IV) prodrugs. In contrast, the Er-UCNPs have strong emission bands at wavelengths very near to or overlapping with the LMCT bands of the diiodio-Pt(IV) complexes (Figure 2B and Figure 4).

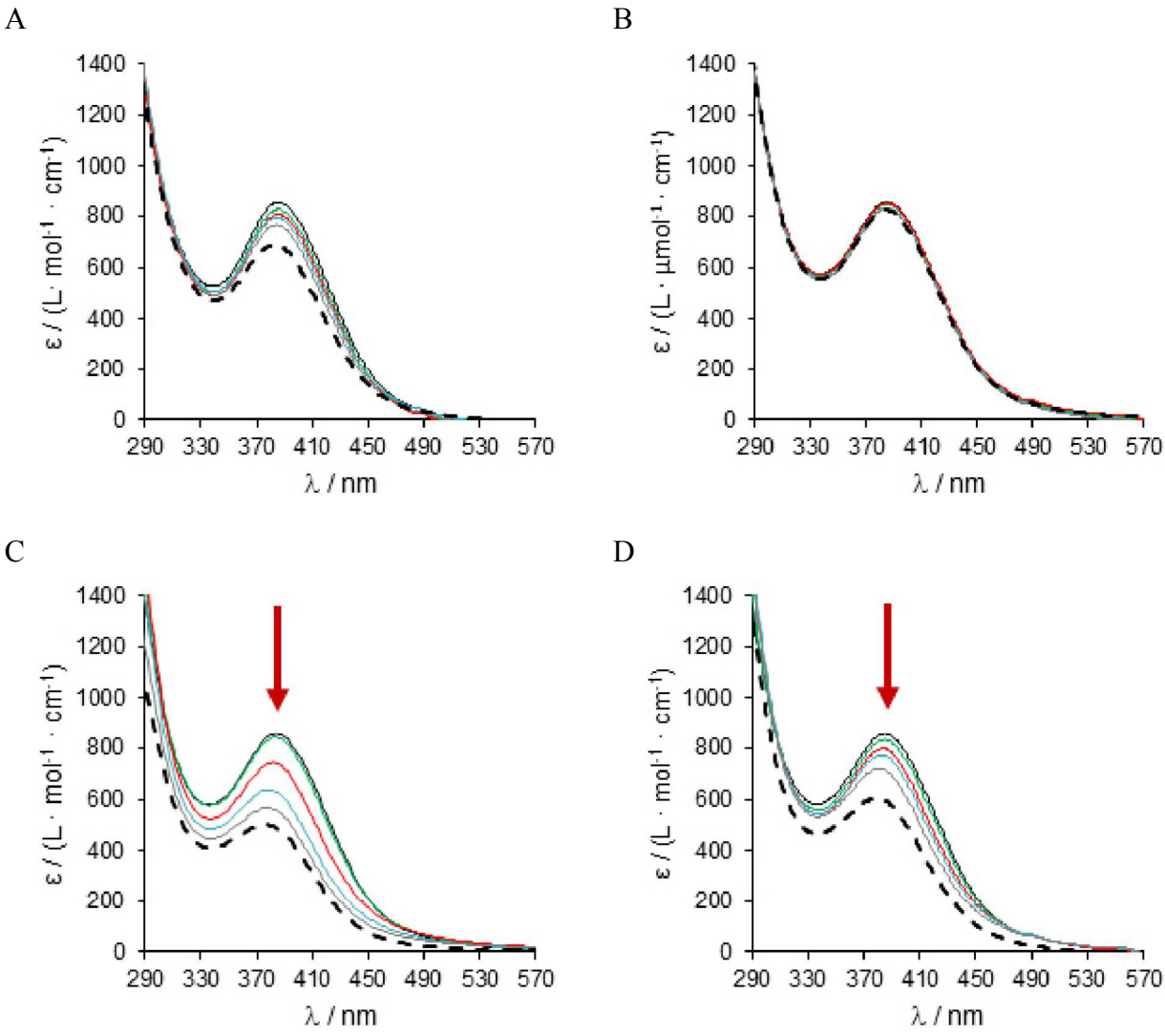

Figure 5. Time-dependent changes in the LMCT-band of complex **2** (500 µM) in the presence of 3 mg/mL oleate-capped UCNPs and NIR (in 10 mM PIPES/$NaClO_4$ buffer, pH 6.9). **A**: irradiated with a 980 nm NIR laser without UCNPs; **B**: dark control in the presence of $NaGdF_4$:Yb,Tm-UCNPs; **C**: with $NaGdF_4$:Yb,Tm-UCNPs, irradiated with NIR laser; **D**: with $NaGdF_4$:Yb,Er-UCNPs, irradiated with NIR laser (time 0: black, 1 h: green, 2 h: red, 3 h: blue, 3.5 h: grey, dashed line: 3.5 h NIR + 20.5 h post irradiation in the dark).

While the results of the above UV/vis studies showed a decrease in the LMCT bands upon irradiation with NIR in the presence of UCNPs, these experiments do not prove that this photodecomposition leads to reactivate Pt species that can interact with biological systems. Nuclear DNA is considered the molecular target of cisplatin when killing cancer cells.[34] Thus, as a proof of mechanism study we tested the ability of NIR light to photoactivate diiodido-Pt(IV) complexes in the presence of $NaGdF_4$:Yb,Er-UCNPs to reactive Pt species that can irreversibly bind to calf thymus DNA (ct-DNA). Simple mixtures of $NaGdF_4$:Yb,Er-UCNPs and Pt complexes **2**, **3** and **4** (Figure 6) were incubated either in the dark or irradiated with a NIR laser, then the pre-activated Pt complexes were mixed with a solution of calf thymus (ct) DNA. The amount of Pt bound irreversibly to ct-DNA at specified times was measured by AAS. As shown in Figure 6, a greater amount of Pt binding to ct-DNA was found when all three complexes were irradiated with NIR for 4 h prior to adding ct-DNA, compared to dark controls. This was particularly apparent with the monosuccinate complex **3**; this complex gave the highest level of DNA platination in the shortest period of time. Nonetheless, there is also appreciable binding of all synthesized Pt complexes to DNA in the non-preactivated dark controls. An explanation for this phenomenon might be that the UCNPs can chemically reduce a fraction of Pt(IV) to Pt(II) (see next section).

A

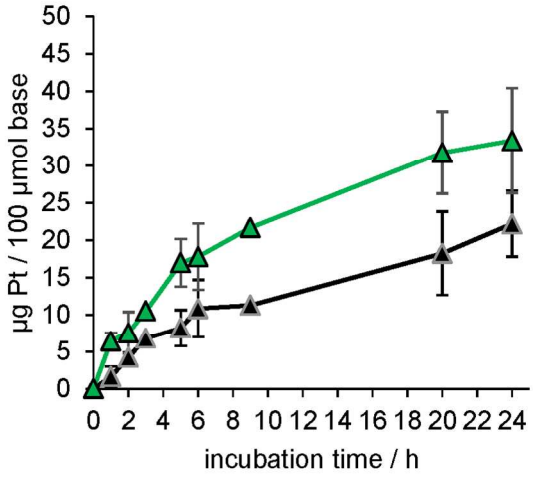

B

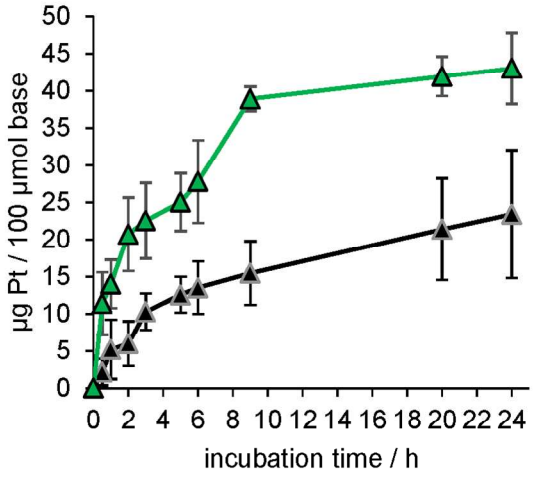

C

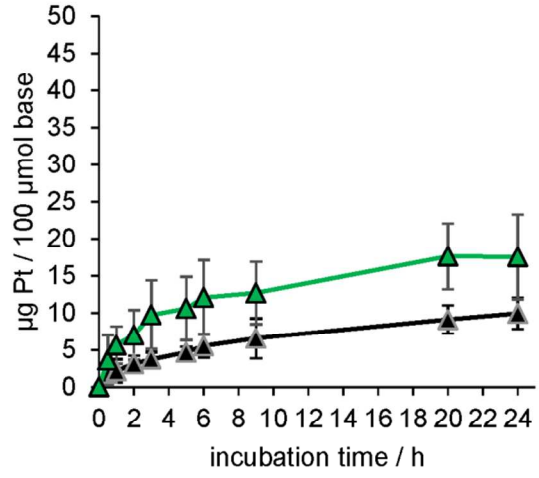

Figure 6. Time-dependent binding of Pt to ct-DNA (average ± standard deviations, n = 3) at 37 °C by NIR activated Pt complexes **2** (A), **3** (B) and **4** (C) (all at 20 µM) in 10 mM PIPES/$NaClO_4$ buffer (pH 6.9). In the presence of 0.8 mg/mL oleate-capped $NaGdF_4$:Yb,Er-UCNPs, the Pt complexes were either kept in the dark (black curve) or irradiated with a 980 nm NIR laser for 4 h (green curve), then centrifuged and the supernatant reacted with 0.25 mg/mL ct-DNA. (t = 0: mixing of pre-activated Pt complex with DNA).

Coupling of diiodido-Pt complexes to UCNPs. To achieve coupling of small molecules to UCNPs, various procedures are available including covalent attachment by amide formation to amino-modified UCNPs and carboxylate ligand exchange at the surface of the UCNP.[35] To attach diiodido-Pt(IV) diamines to UCNPs, we adopted two different strategies, which are displayed in Figure 1. In the first approach (A) (Figure 1A), free carboxylate groups of the axial Pt(IV) ligands in **3** and **4** were used to covalently attach the complex to the amorphous silica shell surface that had been modified with amine groups. (Complex **2** was not utilized for such studies because of limited amounts of material resulting from the poor synthetic yield). Amino-modified $NaGdF_4$:Yb,Er-UCNPs were coupled with Pt complexes **3** and **4** by standard amide formation reaction between carboxyl groups of complex and amino groups on the surface of UCNPs with the aid of 1-ethyl-3-(3-dimethylaminopropyl)carbodiimide (EDC) and *N*-hydroxysuccinimide (NHS). This conjugation method is used, for example, for attaching proteins to UCNPs for imaging of cancer cells.[24] In the second approach (**B**) (Figure 1B), coupling was performed by allowing the oleate molecules on the surface of the UCNPs to be exchanged by the carboxylate ligands of the diiodido-Pt(IV) complexes **3** and **4**. Oleate molecules are attached to the nanoparticles through electrostatic interactions of their carboxylate functions and thus could be displaced by the carboxylate groups of complexes **3** and **4**. To our knowledge, such a strategy of coupling of Pt complexes to UCNPs has not yet been reported. As in approach A, photoreduction of Pt(IV) to Pt(II) followed by aquation should lead to the formation of the cytotoxic $[Pt(en)(H_2O)_2]^{2+}$ (Figure 1).

The degree of coupling of the diiodido-Pt(IV) complexes to the surface of the UCNPs was evaluated by these two methods: AAS analysis of the Pt content of the UCNP and X-ray

photoelectron spectroscopy (XPS). Moreover, XPS analysis allowed to have information on Pt chemical state.

The relative mass of Pt bound to the UCNPs as measure by AAS was found to be ca. 0.15% of the total mass of the modified UCNPs (for $NaGdF_4$:Yb,Er -SiO_2-NH-**3** and $NaGdF_4$:Yb,Er- SiO_2-NH-**4** 1.88 and 1.32 µg Pt/mg UCNP, respectively).

For an accurate XPS analysis of the UCNP-Pt conjugates, the stability of Pt complexes **3** and **4** under the X-ray source was investigated. It was found that the Pt(IV) complexes are slightly unstable to the X-ray beam and are reduced to Pt(II) after prolonged exposure to X-rays. It is worth underlining that minimum time of exposure to obtain an optimal signal/noise ratio (determined by means of repeated measurements at increasing irradiation time) was used to avoid the reduction of Pt(IV) to Pt(II) under XPS conditions. In particular, two acquisitions, performed after 5 and 15 min exposures to X-rays, resulted in no observable changes in Pt 4f core level.

The conjugation of UCNPs with Pt complex by amide bond formation was evaluated first (strategy A in Figure 1). In Figure 8 the XPS spectra of the conjugate $NaGdF_4$:Yb,Er-SiO_2-NH-**3** recorded after 5 min of exposure to X-ray source are shown and compared with those of **3** (after 5 min), [PtI_2(en)] and the amino-modified $NaGdF_4$:Yb,Er-SiO_2-NH_2 before coupling with Pt. These results confirm the presence of Pt, I and N on the surface of UCNP. A careful analysis of the Pt 4f region of the conjugate $NaGdF_4$:Yb,Er-SiO_2-NH-**3** reveals the presence of two doublets (well evident in deconvolution of Pt 4f of $NaGdF_4$:Yb,Er- SiO_2-NH-**3**). The comparison with Pt 4f peak of complex **3** and Pt(II) complex, [PtI_2(en)], suggests that the doublet at lower binding energy (BE) (73.1, 76.4 eV) is characteristic of Pt(II), while the one at higher BEs (74.8, 78.1 eV) is due to Pt(IV) (see Table S2). Same considerations also apply for $NaGdF_4$:Yb,Er- SiO_2-

NH-**4** (see Table S2). The amount of Pt(IV) in conjugate $NaGdF_4$:Yb,Er-SiO_2-NH-**3** is lower than in the pure complex **3** (Figure 8). The deconvolution procedure, in fact, reveals that for both conjugates, $NaGdF_4$:Yb,Er-SiO_2-NH-**3** and $NaGdF_4$:Yb,Er-SiO_2-NH-**4**, the doublet characteristic of Pt(II) is stronger in intensity than the one of Pt(IV) by ca. four fold (see Table S3). Unlike complex **3** no changes of Pt 4f peak are observed in conjugate $NaGdF_4$:Yb,Er-SiO_2-NH-**3** after prolonged exposure to X-ray source. This behavior suggests that the reduction occurred during the coupling reaction and is not an artifact of the measurement. No changes are evident in I 3d region, indicating that iodide coordinated to Pt is present on the surface of the UCNPs (Figure 8). The peak position of O 1s observed in the conjugate is consistent with the presence of oxygen species in the Pt complex and silica. Concerning the N 1s peak, the sample conjugate $NaGdF_4$:Yb,Er-SiO_2-NH-**3** shows a N 1s BE higher than nitrogen in $NaGdF_4$:Yb,Er-SiO_2-NH_2, in which free amino groups are present, suggesting that the main fraction of amino groups on silica shell surface are those from ethylene diamine coordinated with Pt. The Si 2p peak is also shifted to slightly higher BE in the conjugate (Figure 8, Table S2). All these considerations also apply for $NaGdF_4$:Yb,Er- SiO_2-NH-**4** (see Table S2).

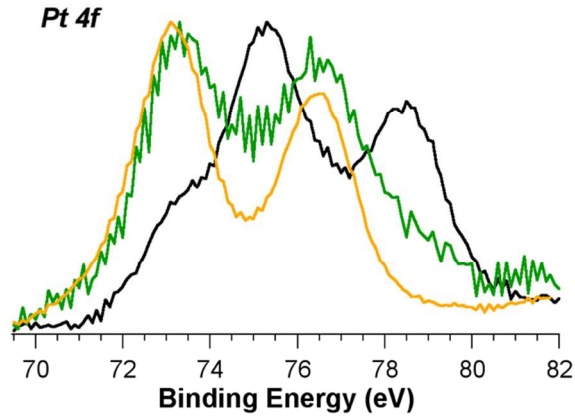
Pt 4f
70
72
74
76
78
80
82
Binding Energy (eV)

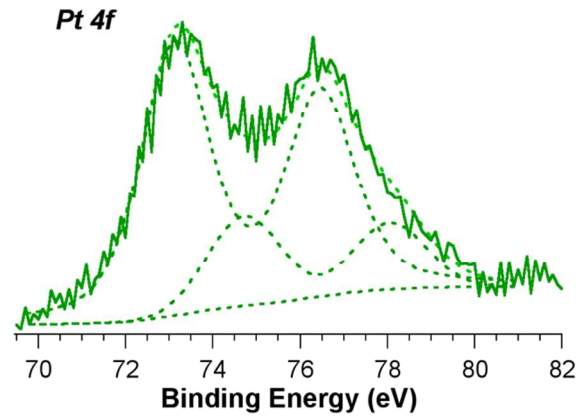
Pt 4f
70
72
74
76
78
80
82
Binding Energy (eV)

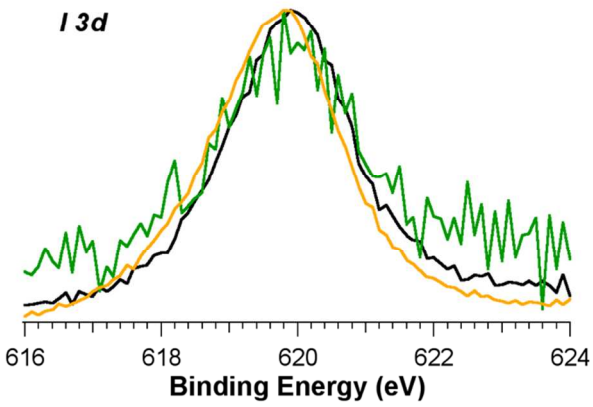
I 3d
616
618
620
622
624
Binding Energy (eV)

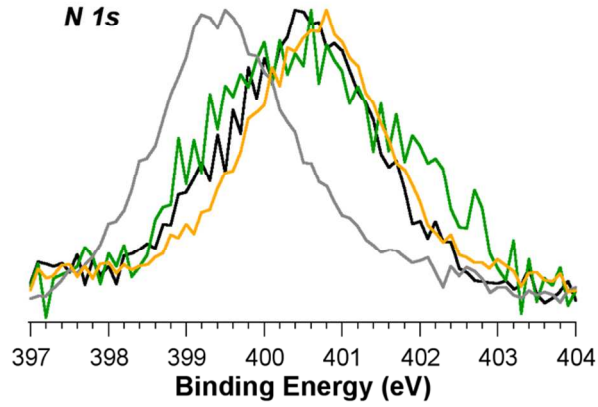
N 1s
397
398
399
400
401
402
403
404
Binding Energy (eV)

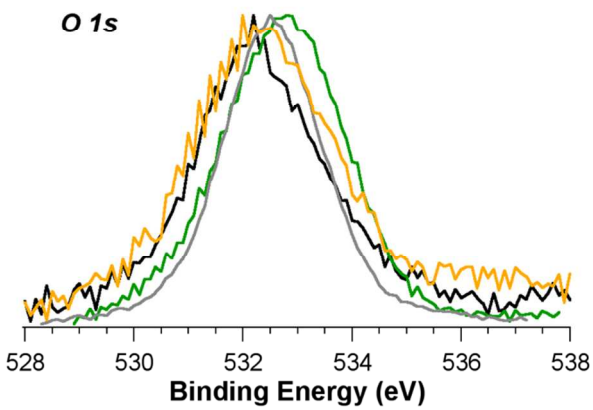
O 1s
528
530
532
534
536
538
Binding Energy (eV)

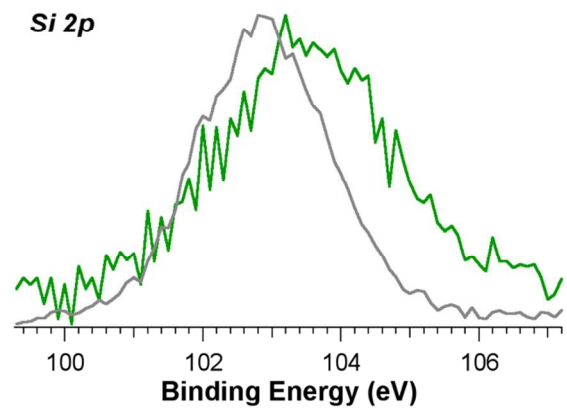
Si 2p
100
102
104
106
Binding Energy (eV)

Figure 8. XPS spectra $NaGdF_4$:Yb,Er-SiO_2-NH-**3**. Pt 4f, I 3d, O 1s, N 1s and Si 2p XPS spectra of $NaGdF_4$:Yb,Er-SiO_2-NH_2 (grey line), covalent conjugate $NaGdF_4$:Yb,Er-SiO_2-NH-**3** (green line), free complexes **3** (black line) and [Pt(II)I_2(en)] (yellow line) after 5 min of exposure at X-ray source; fitting of Pt 4f XPS peak of conjugate $NaGdF_4$:Yb,Er-SiO_2-NH-**3** (dashed line) is reported. Spectra are normalized respect to their maximum and baseline.

The carboxylate constructs (strategy B in Figure 1) were characterized by FTIR, AAS and XPS. By FTIR analysis the exchange of oleate ligands for carboxylated Pt(IV) diamines could be verified; the characteristic bands of oleate have completely disappeared in the FTIR spectrum of $NaGdF_4$:Yb,Er-**4** (Figure S2). The AAS analyses of the two carboxylate constructs of **3** and **4** showed a slightly lower amount of Pt associated with the UCNPs ($NaGdF_4$:Yb,Er-**3** and $NaGdF_4$:Yb,Er-**4** had 1.21 and 1.00 μg Pt/mg UCNP, respectively) compared to covalent conjugates $NaGdF_4$:Yb,Er-SiO_2-NH-**3** and $NaGdF_4$:Yb,Er-SiO_2-NH-**4** (1.88 and 1.32 μg Pt/mg UCNP, respectively).

With the XPS analysis of the carboxylate conjugates, Na and F species (main species in the UCNPs) are also evident in addition to the elements characteristic of the Pt-complex (Pt, I, O and N). In general, the Pt 4f, I 3d, O 1s and N 1s peaks are similar to those observed in the amide conjugate $NaGdF_4$:Yb,Er-SiO_2-NH-**3** but are weaker in intensity; this is consistent with the data from the AAS measurements that indicated somewhat less Pt bound per mg UCNP to the carboxylate constructs compared to the covalent conjugates.

The fitting procedure of the Pt 4f of the $NaGdF_4$:Yb,Er-**3** construct reveals, like the covalent conjugates, that the contributions characteristic of Pt(II) are again more intense than those of Pt(IV) (Figure 9, Table S3). For the $NaGdF_4$:Yb,Tm-**4** construct similar Pt(II)/Pt(IV)

ratios were also observed (Figure S5, Table S3). We conclude that both coupling procedures are capable of attaching the diiodido-Pt(IV) complex to UCNPs but that substantial Pt(IV) reduction to Pt(II) takes place as a result of this procedure, just as with strategy A. Thus, some component of the UCNPs may be promoting the reduction of Pt(IV) because the conditions of the coupling procedures alone to do not affect the stability of the diiodio-Pt(IV) complexes. This would be consistent with the observation made earlier that even in the dark mixtures of UCNPs and diiodido-Pt(IV) complexes result in reactive Pt species that can platinate ct-DNA irreversibly (see Figure 6).

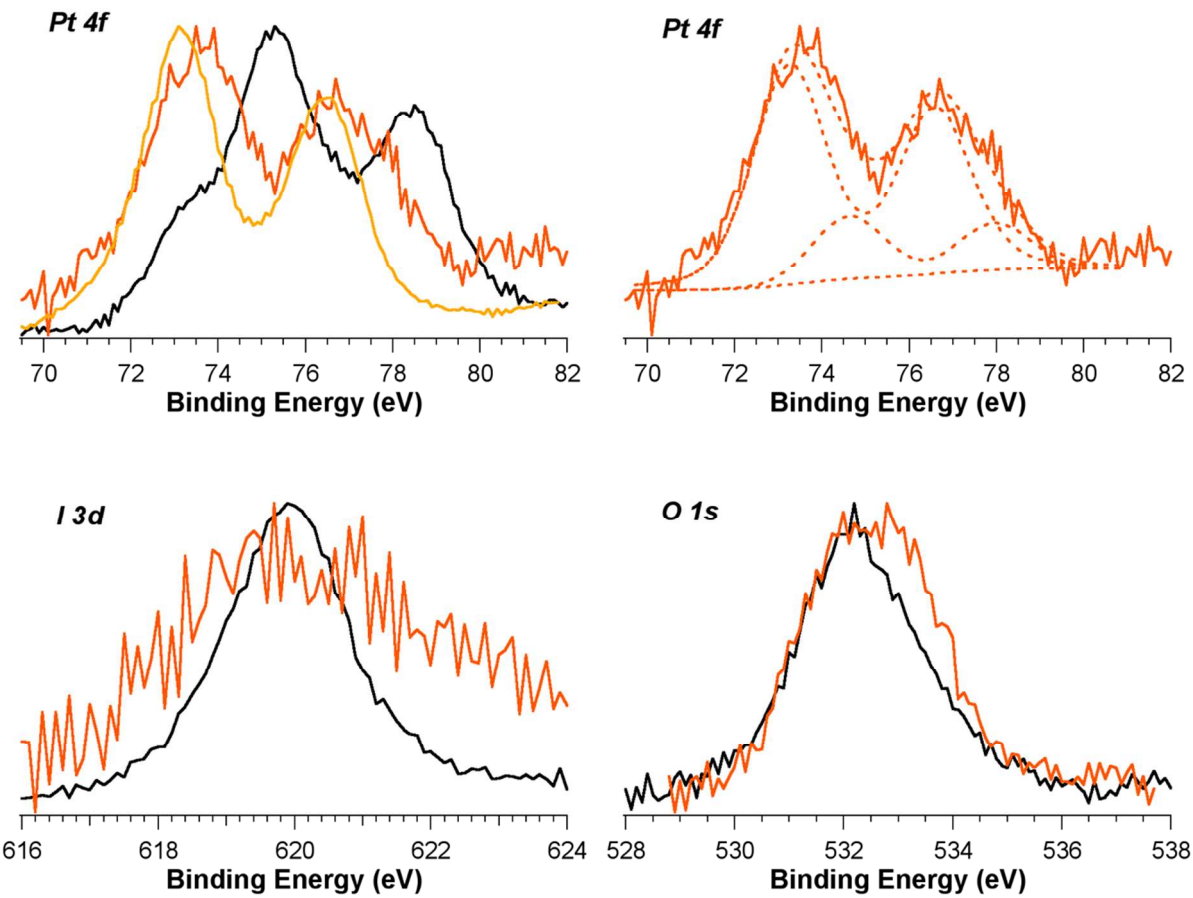

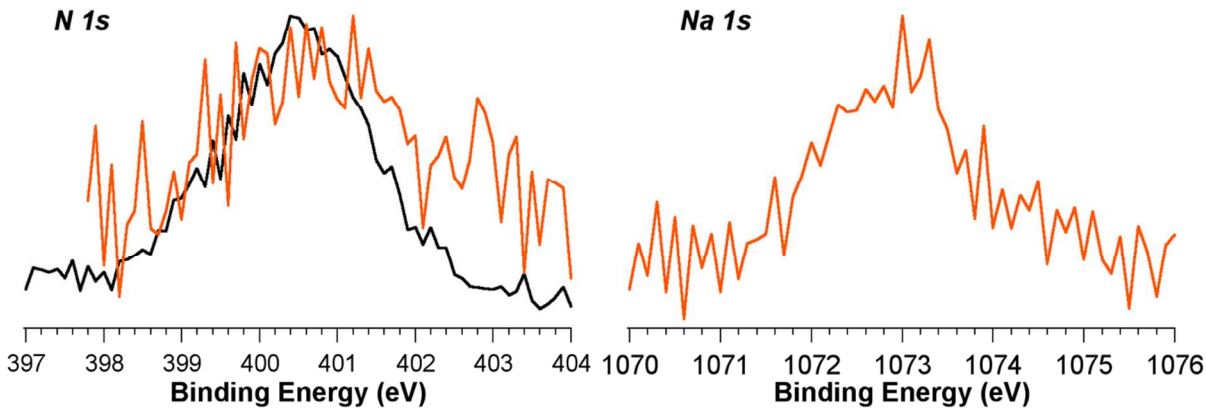

Figure 9. XPS spectra of $NaGdF_4$:Yb,Er-**3.** Pt 4f, I 3d, O 1s, N 1s and Na 1s XPS spectra of the carboxylate construct $NaGdF_4$:Yb,Er-**3** (orange line), complex **3** (black line) and Pt(II)I_2(en) (yellow line) after 5 min of exposure at X-ray source; fitting of Pt 4f XPS peak of construct $NaGdF_4$:Yb,Er-**3** (dashed line) is reported. Spectra are normalized with respect to their maximum and baseline.

We looked for an energy transfer (ET) of emitted light from UCNPs to the diiodido-Pt(IV) complexes with the carboxylate constructs $NaGdF_4$:Yb,Er-**3** and $NaGdF_4$:Yb,Tm-**3** as well as the covalent conjugates $NaGdF_4$:Yb,Er-SiO_2-NH-**3** and $NaGdF_4$:Yb,Er-SiO_2-NH-**4** by comparing the emission spectra of the non-modified with the modified UCNP. However, in none of these cases did we observe a diminishment in the emission intensities at wavelengths were the diiodido-Pt(IV) complexes adsorbed (data not shown). However, this does not rule out that an ET occurred but was just too weak to be detected; diiodido-Pt(IV) complexes have relatively small extinction coefficients (< 2000 L mol^{-1} cm^{-1}) at the emission wavelengths of these UCNPs. Moreover, from XPS it was found that only 20% of the Pt on the surface of the UCNP was in the Pt(IV) oxidation state, which has the strongest light absorbing properties.

NIR facilitated release of Pt from UCNPs. To validate the photolytic release of Pt from the UCNPs, we measured over 24 h the Pt released from two amide conjugates and one carboxylate construct from Yb,Er-doped UCNP when irradiated with NIR for 5 h. (Yb,Tm-doped UCNPs were not investigated in these studies because the emission spectra of the Er-doped UCNPs overlapped better with the LMCT bands of the diiodio-Pt(IV) complexes, promising better ET.) To control for thermal loss of Pt from the UCNPs due to the warming of the solution by NIR, we compared the release of Pt at room temperature and 37 °C without NIR. As shown in Figure 10A and 10B, by raising the incubation temperature from room temperature to 37 °C, some Pt release was observed, evidence that thermal processes minimally affect the release of Pt. Surprisingly, in dark controls the carboxylate construct $NaGdF_4$:Yb,Er-**4** showed much less Pt released than either of the two covalent conjugates of **3** and **4**. (Figure 10A and 10B) On the other hand, compared to the construct $NaGdF_4$:Yb,Er-**4** (Figure 10C), the conjugates $NaGdF_4$:Yb,Er-SiO_2-NH-**3**/**4** (Figure 10B) showed a greater NIR-dependent release of Pt over the same incubation time. Thus, the NIR-dependent release of Pt is most efficient when the glutarato Pt(IV) complex **4** is covalently attached to UCNPs via amide bonds.

The amounts of Pt released from the modified UCNP conjugates/constructs were compared with the amounts of Pt loaded on the respective UCNPs, as determined by AAS, in order to assess the efficiency of Pt release from the modified UCNPs. It was calculated that, when irradiated with NIR, conjugates $NaGdF_4$:Yb,Er-SiO_2-NH-**3** and $NaGdF_4$:Yb,Er-SiO_2-NH-**4** release 45 and 90% of the total Pt over 24 h, respectively, while NIR irradiated construct $NaGdF_4$:Yb,Er-**4** releases just 30% of its total Pt over 24 h.

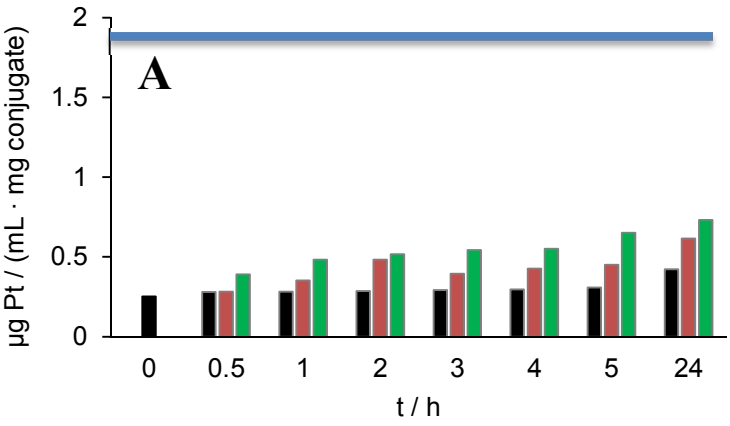
A
µg Pt / (mL · mg conjugate)
2
1.5
1
0.5
0
0
0.5
1
2
3
4
5
24
t / h

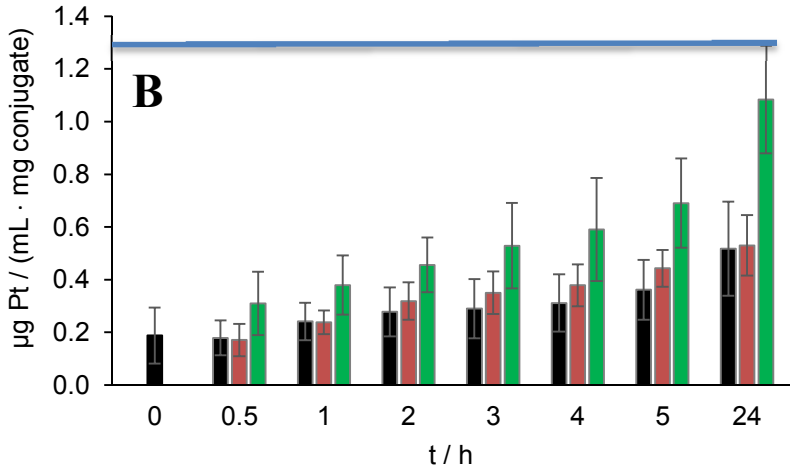
B
µg Pt / (mL · mg conjugate)
1.4
1.2
1.0
0.8
0.6
0.4
0.2
0.0
0
0.5
1
2
3
4
5
24
t / h

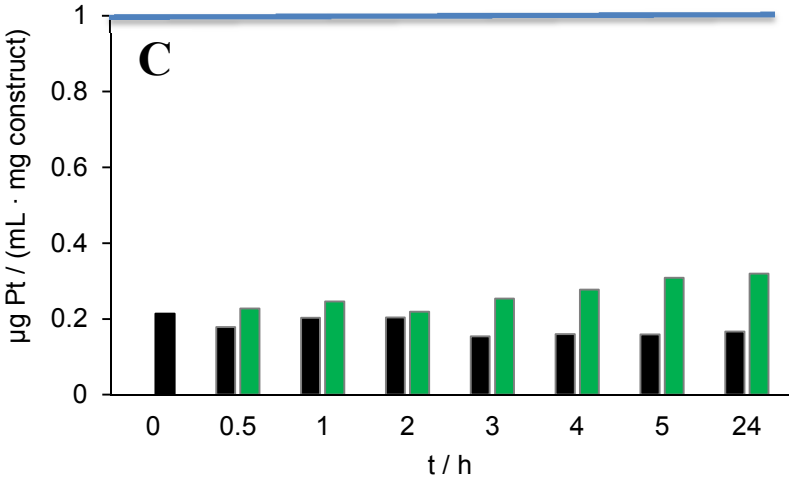
C
µg Pt / (mL · mg construct)
1
0.8
0.6
0.4
0.2
0
0
0.5
1
2
3
4
5
24
t / h

Figure 10. Platinum release from three types of UCNPs (0.5 mg/mL), determined by AAS, under varying conditions. **A**: covalent conjugate $NaGdF_4$:Yb,Er-SiO_2-NH-**3** (n = 2); **B**: covalent conjugate $NaGdF_4$:Yb,Er-SiO_2-NH-**4** (n = 5); **C**: carboxylate construct $NaGdF_4$:Yb,Er-**4** (n = 2); dark controls at room temperature (black), dark controls at 37 °C (red), irradiation with 980 nm laser for 5 h (green) in 10 mM PIPES/$NaClO_4$ buffer (pH 6.9) and then incubated in the dark for an additional 19 h at the respective temperature. The upper blue line represents the 100% theoretical level of Pt that could be released, based on the loading level of Pt for the respective UCNPs.

NIR facilitated release of Pt from UCNPs and binding to ct-DNA.

We next investigated whether the released Pt was capable of interacting irreversibly with ct-DNA, which was added to the supernatant of centrifuged samples of the covalently modified conjugate $NaGdF_4$:Yb,Er-SiO_2-NH-**3** after it was irradiated with NIR for 4 h. Figure 11 shows a noticeable increase in platinated ct-DNA already after a 2 h irradiation compared to samples held in the dark. By 6 h the levels of Pt bound to DNA were nearly 3 times greater in the irradiated samples compared to dark controls. However, by 24 h these differences were largely mitigated due to the slow release and binding of Pt to ct-DNA in the dark controls. These results demonstrate that the Pt released from covalently modified UCNPs is still chemically reactive enough to bind to DNA and that a kinetic advantage for Pt release exists when irradiation is done with NIR.

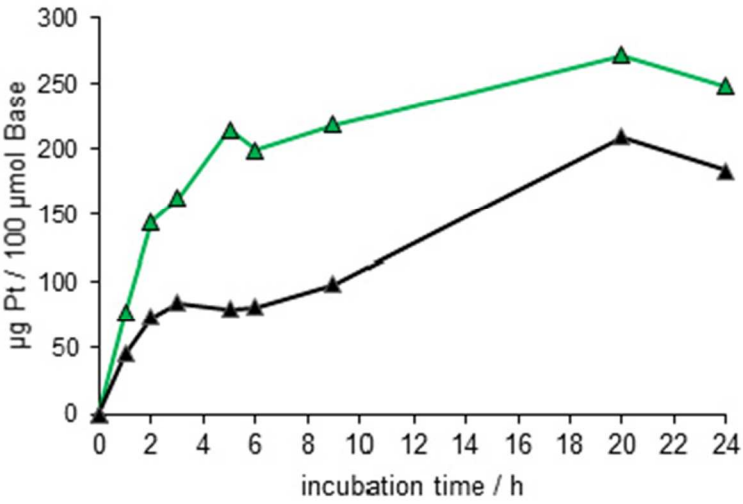

Figure 11. Time-dependent irreversible binding of Pt to ct-DNA after 4 h NIR activation of the $NaGdF_4$:Yb,Er-SiO_2-NH-**3** conjugate. Samples were either pre-irradiated for 4 h with a 980 nm laser (green) or kept in the dark (black), then centrifuged and the supernatant reacted with 0.25 mg/mL ct-DNA in PIPES/$NaClO_4$ buffer (pH 6.9) at 37 ° C for the times shown in the diagram.

Effects of NIR on the cytotoxicity of UCNPs coupled to diiodido-Pt(IV) complexes.

Finally, cell experiments were performed to test the cytotoxic potential of the modified UCNPs with and without light irradiation with NIR. For these studies, the human leukemia cell lines HL60 was used because the cells grow in suspension and thus allow for a homogeneous irradiation of the stirred cell suspension by a NIR laser. In Figure 12 the cytotoxicity caused by Yb,Er-doped UCNP conjugates or constructs, with and without irradiation with a 980 nm laser are compared. All four UCNP conjugates/constructs became significantly more active when treatment was accompanied by NIR, whereby covalent conjugate $NaGdF_4$:Yb,Er-SiO_2-NH-**4**

showed the greatest cytotoxicity (Figure 12D IV). However, the two covalent conjugates $NaGdF_4$:Yb,Er-SiO_2-NH-**3**/**4** also showed more dark toxicity than the two carboxylate constructs $NaGdF_4$:Yb,Er-**3**/**4** (compare II in A–D). This may be a result of the greater loss of Pt in the dark from the UCNP conjugates as opposed to the constructs, as indicated in Figure 10. The dose of NIR used in this protocol negatively affected cell viability in the absence of UCNPs, showing a ca. 70 % decrease in cell viability compared to cells kept in the dark. However, due to the fact that cytotoxicity of the UCNPs coupled with Pt complexes is much greater when irradiated only with NIR, this boost in cytotoxicity could be attributed to the UCNP conjugates/constructs.

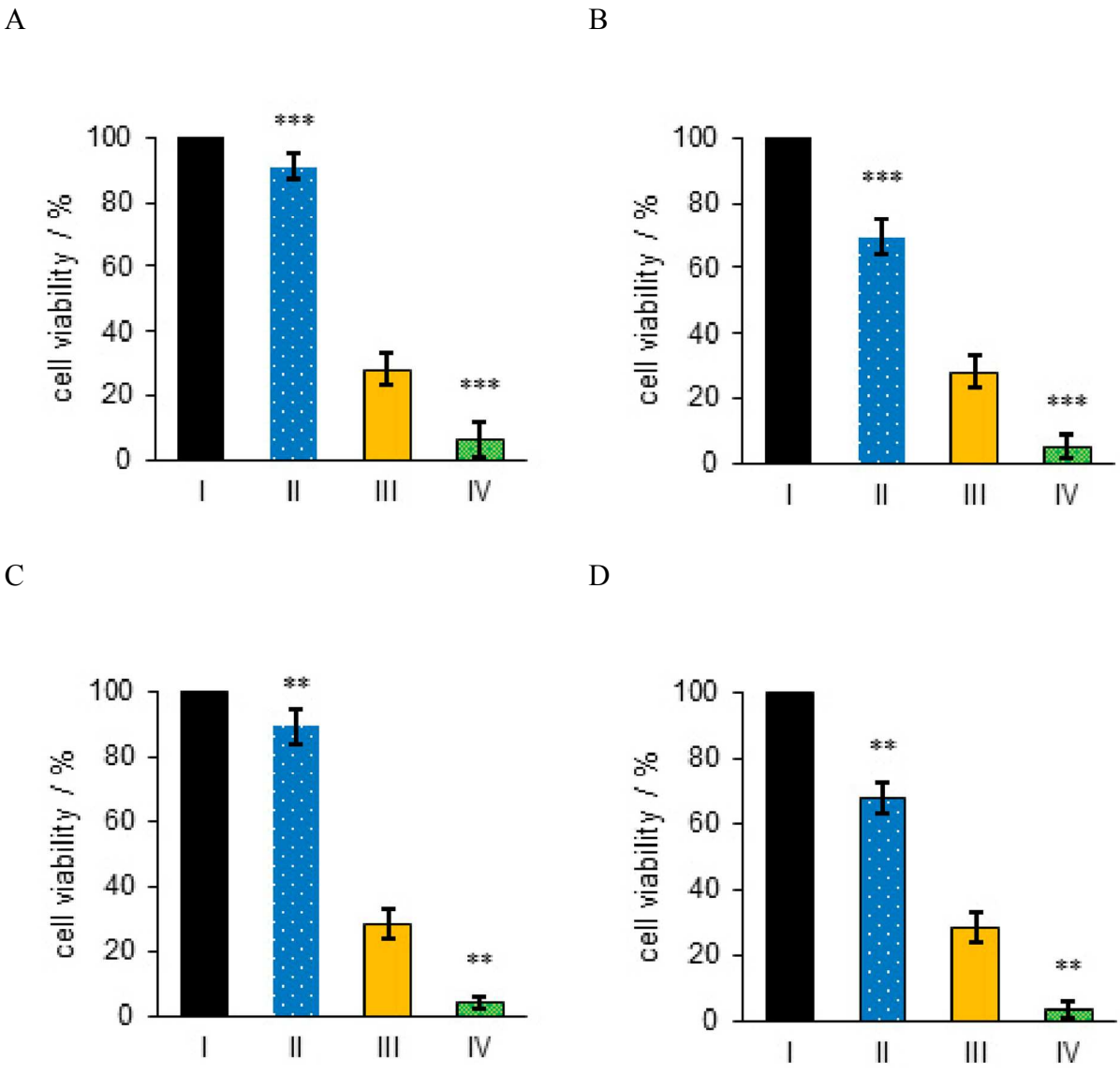

Figure 12. Cytotoxicity in HL60 cells in the presence of Er-doped UCNP conjugates/constructs (0.1 mg/mL) and NIR light λ = 980 nm (30 min NIR, 15 min dark, repeated five times). **A**: carboxylate construct $NaGdF_4$:Yb,Er-**3**, **B**: covalent conjugate $NaGdF_4$:Yb,Er-SiO_2-NH-**3**, **C**: carboxylate construct $NaGdF_4$:Yb,Er-**4** and **D**: covalent conjugate $NaGdF_4$:Yb,Er-SiO_2-NH-**4**. I: untreated control in dark; II: UCNPs in dark; III: NIR; IV: UCNPs + NIR. Experiments show averages and standard deviations of 3 independent experiments; significance determined by two-sided, paired t-test, $^{**}p < 0.01$, $^{***}p < 0.001$.

Discussion

Yb,Er- and Yb,Tm-doped β–$NaGdF_4$ with crystallite diameter of ca. 50 nm, able to up-convert by NIR (λ = 980 nm) to UV-vis light were prepared. The emission spectra of the UCNPs, excited by a 980 nm laser, and the absorption spectra of the diiodido-Pt(IV) derivatives overlap at various wavelengths (Figure 4), suggesting that the coupling of these two structures might provide a method for photoactivating the Pt(IV) prodrugs with NIR, which can penetrate deeper into tumor tissues than visible light. Two different strategies were compared for linking photoactivatable diiodido-Pt(IV) antitumor prodrugs to UCNPs. For this purpose, two derivatives of *trans,cis*-[$Pt(OH)_2I_2(en)$] were prepared with either succinato or glutarato ligands in the axial position to enable attachment to the UCNPs by two strategies: A) covalent bonding by amide formation and B) by carboxylate exchange (Figure 1).

Even without UCNPs, most of the synthesized diiodido-Pt(IV) derivatives (**2**–**4** were photoactivated by either UVA or visible light, resulting in several cases in significant reductions in the IC_{50} values with various human cancer cell lines compared to dark controls (Tables 1 and 2). (The exception was complex **4** in the HL60 cell line, where the IC_{50} value was lower in the dark compared to the UVA irradiated experiment.). Nevertheless, the differences between IC_{50} values from light and dark experiments were small and only in the range of 8–50%; this is because diiodido-Pt(IV) prodrugs can also be efficiently activated in cell culture in the dark. Similar results were observed previously for *trans,cis*-[$Pt(OAc)_2I_2(en)$].[16]

It could be shown in a feasibility study that the addition of UCNPs to solutions of diiodido-Pt(IV) derivatives resulted in a decrease in the intense LMCT bands, characteristic of

the iodido-Pt(IV) bond, when the solutions were irradiated with a 980 nm laser, while the laser alone had only a minimal effect on the stability of the complexes and the presence of the UCNP in the dark had no effect (Figure 5). The presented experiments were mostly performed with Yb,Er-doped $NaGdF_4$-UCNPs instead of the Tm-doped counterpart because the wavelengths of emitted light from the Er-doped UCNP overlapped better with the LMCT bands of the diiodido-Pt(IV) complexes, promising a more efficient ET. (Figure 4)

The platinum that was photolyzed during this process was capable of binding irreversibly to ct-DNA, further evidence that a reduction from Pt(IV) to Pt(II) had taken place (Figure 6). Nonetheless, even without irradiation with NIR, a substantial binding of Pt to ct-DNA was observed, evidence that some type of nonspecific activation process was also taking place.

Thus, a further motivation for attaching photosensitive Pt(IV) diamines to UCNPs was to increase the chemical stability and prevent premature activation in biological media. However, as shown here, this goal was not fulfilled. In fact, the UCNPs themselves appeared to enhance the reduction of Pt(IV) to Pt(II), as seen in the XPS data; the XPS showed that for both covalently modified as well as carboxylate exchange UCNPs only about 20 % of the Pt was in the Pt(IV) oxidation state following coupling, the rest being Pt(II) (Figures 8 and 9, respectively). The X-ray bombardment during the XPS analysis could be ruled out as a main source of Pt(IV) reduction. A XPS signal from the I 3d region was a further confirmation that the diiodio-Pt(IV) complexes were indeed present on the UCNPs. Although there is still work to do to better understand the source of Pt reduction, we believe that some components of the UCNPs may be promoting the reduction of Pt(IV). As a matter of fact, the conditions of the coupling procedure alone do not seem to affect the stability of the diiodio-Pt(IV) complexes; both amino-modified as well as the carboxylate- exchanged UCNPs had similar ratios of Pt(IV) to Pt(II). (Table 3S)

Ruggiero and coworkers observed only Pt(IV) by XPS when dichorido-P(IV) diamines were attached to $NaYF_4:Yb^{3+},Tm^{3+}$ core UCNPs.[14] The contrasting stability between dichlorido and diiodido is most likely due to the lower reduction potentials of diiodido-Pt(IV) compared to dichloride-Pt(IV) diamines.[36]

To assess the photoactivation of the diiodido-Pt(IV) diamines linked to UCNPs, the rates of release of Pt from the UCNP were measured by AAS. Stirred suspensions of the three UCNP forms were irradiated with a 980 nm laser for various times up to 4 h, after which the suspensions were centrifuged and the Pt content of the supernatants measured. It was found that the covalently conjugated UCNPs most effectively released Pt into the solution during irradiation (Figure 10A and 10B). The carboxylate exchange construct was much less efficient (Figure 10C). The Pt(II) diamines that would be expected to form in the photoreduction from both the carboxylate exchange construct and the covalent conjugate would be Pt(II) monocarboxylates (Figure 1), which following aquation would result in release of cytotoxic $[Pten(H_2O)_2]^{2+}$ and diffuse into the aqueous phase. In dark controls, little differences in Pt release from the UCNPs were observed when the temperature was raised from RT to 37 °C, evidence that the increased Pt released during irradiation with NIR was not simply a result of thermals effects (Figure 10A and 10B).

Surprisingly, the carboxylate construct $NaGdF_4:Yb,Er$-**4** showed less Pt release in the dark compared to either covalent conjugate (Figure 9), although the ionic bonds holding the carboxylate groups to the UCNPs are assumed to be weaker than the covalent amide bonds holding Pt to the nanoparticles $NaGdF_4:Yb,Er$-SiO_2-NH-**3/4**. While both carboxylate constructs contained somewhat less Pt per mg UCNP compared to the covalent conjugates, as determined by AAS, this difference can not account for the much lower release of Pt from the construct

$NaGdF_4$:Yb,Er-**4**. A possible explanation could be that the silicate shell of the covalent conjugate UCNPs leads to better water dispersablity, thus making the Pt on the surface more chemically reactive towards water, which is required for the release of Pt(II) from the UCNP (see Figure 1).

The phototoxicity of the new diiodido-Pt(IV) modified UCNPs was investigated to determine if NIR is capable of increasing the toxicity of the UCNPs. For these studies, a human leukemia cell line HL60 was used because this cell line grows in suspension and can be stirred in a culture vessel during the irradiation with a laser, thus affording for homogenous drug activation. When a 30 min irradiation with the 980 nm laser was repeated five times with a 15 min dark interval in between, near total cytotoxicities for all four forms of the Pt(IV) modified UCNPs at 0.1 mg/ml were achieved (Figure 12). With this irradiation scheme, the conjugate NaGdF4:Yb,Er-SiO_2-NH-**4** showed the greatest level of phototoxicity. We conclude that amide conjugation appears to be the more favorable strategy to attach diiodido-Pt(IV) prodrugs to UCNPs. This conclusion is also based on the stronger Pt release of covalent conjugates compared to the carboxylate construct in the presence of NIR (Figure 10). Nonetheless, the carboxylate construct has the advantage that its cytotoxicity is lower in the dark (Figure 12). The irradiation scheme used here alone (e.g., without UCNPs) resulted in a 70 % reduction in cell vitality; such toxicity was most probably a result of photothermal effects due to the temperature of the incubations rising to ca. 40 °C by the end of each 30 min irradiation.

Conclusion

The present work is the first example for nano-hybrids consisting of UCNPs coupled to highly light-sensitive diiodido-Pt(IV) complexes. NIR (λ = 980 nm) up-converting $NaGdF_4$:Yb,Er(or

Tm) nanoparticles cause photolytic decomposition of all diiodido-Pt(IV) complexes, marked by the reduction in the intensity of the LMCT bands in the UV/vis spectra. The usefulness of the amino-modified UCNPs as well as oleate-capped to form nano-hybrids with light-sensitive diiodido-Pt(IV) complexes (strategies **A** and **B**) was evidenced by AAS and XPS analyses; both strategies lead to comparable relative amounts of Pt loaded on the UCNPs, however, only about 20% of the Pt on the surface of the UCNP was in the Pt(IV) state. NIR brought about a noticeable release of Pt from the surface of the covalently modified UCNPs compared to dark controls (strategy **A**) but comparatively little release from the non-covalently modified constructs produced by strategy **B** was measured. Covalent binding Pt to DNA in the photolysized samples of the covalently modified UCNP was observed but Pt also became bound to DNA in dark controls, albeit at a slower rate. The cytotoxicity studies with UCNP conjugates/constructs showed that an overall irradiation time of 3 h led to highly significant decreases in cell viability, but the toxic effects of NIR laser alone were also not negligible, presumably because of thermal warming of the cultures. Thus, covalent conjugates of UCNPs with diiodio-Pt(IV) complexes modified by both strategies **A** and **B** have features attractive for use in PACT, but before these methods can be fully exploited, procedures for attaching diiodido-Pt(IV) complexes to the UCNPs must be developed that do not cause significant reduction of Pt(IV) to Pt(II).

Acknowledgements

We wish to acknowledge COST Action CM1105 for providing SP with a STSM, as well as all members of the action for useful discussions. HSM was supported by the German Ministry of Education and Research (BMBF) within the project FKZ 03Z2CN11 (ZIK HIKE). MMN acknowledges Prof. L. Armelao and Prof A. Glisenti for their support and useful discussions. We

are grateful to Dr. Harm Wulff for performing preliminary XRD measurements, Dr. Anja Bodtke for performing NMR and some MS measurements and Ms. Anne Schüttler for technical assistance. We also would like to thank the reviewers for their very helpful and constructive comments.

Supporting Information. Figures S1–S4 and Tables S1–S3. This material is available free of charge via the Internet at "http://pubs.acs.org."

Author Contributions

SP synthesized Pt(IV) complexes, coupled Pt complexes to UCNPs, and measured NIR facilitated Pt release, Pt-DNA binding and cytoxicity. MMN contributed to the conception of the study, prepared UCNPs and performed TEM, XRD, XPS and up-conversion studies. HSM supported SP concerning the NIR-mediated photoactivation studies of diiodido-Pt complexes by UV/vis spectroscopy. CAH led XRD measurements on UCNPs. CS performed structural analysis of the Pt complexes. GN led synthesis of Pt(IV) carboxylates. PJB conceived the research idea, planned research project, organized collaborations, supervised progress and measured amount of Pt bound to UCNPs by AAS.

Funding Sources

This work was supported by European Research Council (BioIncmed 247450) and the Italian Ministero dell'Università (PON01_01078 and FIRB RINAME RBAP114AMK).

Abbreviations

AAS, atomic absorption spectroscopy; ATR-FTIR, attenuated total reflection-Fourier transform infrared spectroscopy; ct-DNA, calf thymus DNA; DMF, *N,N*-dimethyl formamide; DMSO, dimethyl sulfoxide; DSC-TGA, differential scanning calorimetry-thermal gravimetric analysis; EDC, 1-ethyl-3-(3-dimethylaminopropyl)-carbodiimide; ET, energy transfer; LMCT, ligand-to-metal charge-transfer; MTT, 3-(4,5-dimethylthiazol-2-yl)-2,5-diphenyltrazolium bromide; NHS, *N*-hydroxysuccinimide; NIR, near infrared; NMR, nuclear magnetic resonance spectroscopy; OA, oleate; OD, optical density; PACT, photoactivated chemotherapy; PIPES, piperazine-*N,N*′-bis(2-ethanesulfonic acid); RT, room temperature; TEM, transmission electron microscopy; UCNPs, upconverting nanoparticles; UVA, ultraviolet A; XPS, X-ray photoelectron spectroscopy; XRD, X-ray diffraction.

References

1. Farrer, N. J.; Salassa, L.; Sadler, P. J. Photoactivated chemotherapy (PACT): the potential of excited-state d-block metals in medicine. *Dalton Trans.* **2009**, 10690-10701.
2. Bednarski, P. J.; Mackay, F. S.; Sadler, P. J. Photoactivatable platinum complexes. *Anticancer Agents Med Chem.* **2007,** *7*, 75-93.
3. Ciesienski, K. L.; Franz, K. J. Keys for unlocking photolabile metal-containing cages. *Angew Chem Int Ed Engl.* **2011,** *50*, 814-824.
4. Berners-Price, S. J. Activating platinum anticancer complexes with visible light. *Angew Chem Int Ed Engl.* **2011,** *50*, 804-805.
5. Shaili, E.; Fernandez-Gimenez, M.; Rodriguez-Astor, S.; Gandioso, A.; Sandin, L.; Garcia-Velez, C.; Massaguer, A.; Clarkson, G. J.; Woods, J. A.; Sadler, P. J.; Marchan, V. A Photoactivatable Platinum(IV) Anticancer Complex Conjugated to the RNA Ligand Guanidinoneomycin. *Chemistry-a European Journal.* **2015,** *21*, 18474-18486.
6. Gandioso, A.; Shaili, E.; Massaguer, A.; Artigas, G.; Gonzalez-Canto, A.; Woods, J. A.; Sadler, P. J.; Marchan, V. An integrin-targeted photoactivatable Pt(IV) complex as a selective

anticancer pro-drug: synthesis and photoactivation studies. *Chemical Communications.* **2015,** *51*, 9169-9172.
7. Kasparkova, J.; Kostrhunova, H.; Novakova, O.; Krikavova, R.; Vanco, J.; Travnicek, Z.; Brabec, V. A Photoactivatable Platinum(IV) Complex Targeting Genomic DNA and Histone Deacetylases. *Angewandte Chemie-International Edition.* **2015,** *54*, 14478-14482.
8. Jacques, S. L. Optical properties of biological tissues: a review. *Physics in Medicine and Biology.* **2013,** *58*, R37-R61.
9. Yang, D.; Ma, P.; Hou, Z.; Cheng, Z.; Li, C.; Lin, J. Current advances in lanthanide ion (Ln(3+))-based upconversion nanomaterials for drug delivery. *Chem Soc Rev.* **2015,** *44*, 1416-1448.
10. Cheng, L.; Wang, C.; Liu, Z. Upconversion nanoparticles and their composite nanostructures for biomedical imaging and cancer therapy. *Nanoscale.* **2013,** *5*, 23-37.
11. Wolfbeis, O. S. An overview of nanoparticles commonly used in fluorescent bioimaging. *Chem Soc Rev.* **2015,** *44*, 4743-4768.
12. Chen, G.; Agren, H.; Ohulchanskyy, T. Y.; Prasad, P. N. Light upconverting core-shell nanostructures: nanophotonic control for emerging applications. *Chem Soc Rev.* **2015,** *44*, 1680-1713.
13. Auzel, F. Upconversion and anti-Stokes processes with f and d ions in solids. *Chem Rev.* **2004,** *104*, 139-173.
14. Haase, M.; Schafer, H. Upconverting nanoparticles. *Angew Chem Int Ed Engl.* **2011,** *50*, 5808-5829.
15. Wang, F.; Liu, X. Recent advances in the chemistry of lanthanide-doped upconversion nanocrystals. *Chemical Society Reviews.* **2009,** *38*, 976-989.
16. Dong, H.; Sun, L.-D.; Yan, C.-H. Energy transfer in lanthanide upconversion studies for extended optical applications. *Chemical Society Reviews.* **2015,** *44*, 1608-1634.
17. Dai, Y.; Xiao, H.; Liu, J.; Yuan, Q.; Ma, P.; Yang, D.; Li, C.; Cheng, Z.; Hou, Z.; Yang, P.; Lin, J. In vivo multimodality imaging and cancer therapy by near-infrared light-triggered trans-platinum pro-drug-conjugated upconverison nanoparticles. *J Am Chem Soc.* **2013,** *135*, 18920-18929.
18. Min, Y.; Li, J.; Liu, F.; Yeow, E. K.; Xing, B. Near-infrared light-mediated photoactivation of a platinum antitumor prodrug and simultaneous cellular apoptosis imaging by upconversion-luminescent nanoparticles. *Angew Chem Int Ed Engl.* **2014,** *53*, 1012-1016.
19. Ruggiero, E.; Hernandez-Gil, J.; Mareque-Rivas, J. C.; Salassa, L. Near infrared activation of an anticancer Pt(IV) complex by Tm-doped upconversion nanoparticles. *Chem Commun (Camb).* **2015,** *51*, 2091-2094.
20. Kratochwil, N. A.; Bednarski, P. J.; Mrozek, H.; Vogler, A.; Nagle, J. K. Photolysis of an iodoplatinum(IV) diamine complex to cytotoxic species by visible light. *Anti-Cancer Drug Design.* **1996,** *11*, 155-171.
21. Kratochwil, N. A.; Zabel, M.; Range, K. J.; Bednarski, P. J. Synthesis and X-ray crystal structure of trans,cis-[Pt(OAc)(2)I-2(en)]: A novel type of cisplatin analog that can be photolyzed by visible light to DNA-binding and cytotoxic species in vitro. *J Med Chem.* **1996,** *39*, 2499-2507.
22. Bogdan, N.; Vetrone, F.; Ozin, G. A.; Capobianco, J. A. Synthesis of Ligand-Free Colloidally Stable Water Dispersible Brightly Luminescent Lanthanide-Doped Upconverting Nanoparticles. *Nano Letters.* **2011,** *11*, 835-840.

23. Mi, C. C.; Tian, Z. H.; Cao, C.; Wang, Z. J.; Mao, C. B.; Xu, S. K. Novel Microwave-Assisted Solvothermal Synthesis of NaYF4:Yb,Er Upconversion Nanoparticles and Their Application in Cancer Cell Imaging. *Langmuir.* **2011,** *27*, 14632-14637.
24. Wang, M.; Mi, C. C.; Wang, W. X.; Liu, C. H.; Wu, Y. F.; Xu, Z. R.; Mao, C. B.; Xu, S. K. Immunolabeling and NIR-Excited Fluorescent Imaging of HeLa Cells by Using NaYF4:Yb,Er Upconversion Nanoparticles. *Acs Nano.* **2009,** *3*, 1580-1586.
25. Dhar, S.; Daniel, W. L.; Giljohann, D. A.; Mirkin, C. A.; Lippard, S. J. Polyvalent Oligonucleotide Gold Nanoparticle Conjugates as Delivery Vehicles for Platinum(IV) Warheads. *J Am Chem Soc.* **2009,** *131*, 14652-14653.
26. Shirley, D. A. High-Resolution X-Ray Photoemission Spectrum of Valence Bands of Gold. *Physical Review B.* **1972,** *5*, 4709-4714.
27. Moulder, J. F.; Stickle, W. F.; Sobol, P. E.; Bomben, K. D., Physical Electronics. In *Handbook of X-ray Photoelectron Spectroscopy*, Chastain, J., Ed. Perkin-Elmer Coorporation: Eden Prairie, Minnesota, 1992.
28. Bednarski, P. J.; Grunert, R.; Zielzki, M.; Wellner, A.; Mackay, F. S.; Sadler, P. J. Light-activated destruction of cancer cell nuclei by platinum diazide complexes. *Chemistry & Biology.* **2006,** *13*, 61-67.
29. Westendorf, A. F.; Zerzankova, L.; Salassa, L.; Sadler, P. J.; Brabec, V.; Bednarski, P. J. Influence of pyridine versus piperidine ligands on the chemical, DNA binding and cytotoxic properties of light activated trans,trans,trans-[Pt(N3)2(OH)2(NH3)(L)]. *Journal of Inorganic Biochemistry.* **2011,** *105*, 652-662.
30. Navas, F.; Perfahl, S.; Garino, C.; Salassa, L.; Novakova, O.; Navarro-Ranninger, C.; Bednarski, P. J.; Malina, J.; Quiroga, A. G. Increasing DNA reactivity and in vitro antitumor activity of trans diiodido Pt(II) complexes with UVA light. *Journal of Inorganic Biochemistry.* **2015**.
31. Bracht, K.; Boubakari; Grunert, R.; Bednarski, P. J. Correlations between the activities of 19 anti-tumor agents and the intracellular glutathione concentrations in a panel of 14 human cancer cell lines: comparisons with the National Cancer Institute data. *Anti-Cancer Drugs.* **2006,** *17*, 41-51.
32. Mosmann, T. Rapid Colorimetric Assay for Cellular Growth and Survival - Application to Proliferation and Cyto-Toxicity Assays. *Journal of Immunological Methods.* **1983,** *65*, 55-63.
33. Naumkin A.V., K.-V. A., Gaarenstroom S. W., Powell C. J., NIST Standard reference Database 20. National Institute of Standards and Technology: Gaithersburg, 2012; 'Vol.' Version 4.1.
34. Jamieson, E. R.; Lippard, S. J. Structure, recognition, and processing of cisplatin-DNA adducts. *Chem Rev.* **1999,** *99*, 2467-2498.
35. Sedlmeier, A.; Gorris, H. H. Surface modification and characterization of photon-upconverting nanoparticles for bioanalytical applications. *Chem Soc Rev.* **2015,** *44*, 1526-1560.
36. Kratochwil, N. A.; Bednarski, P. J. Effect of thiols exported by cancer cells on the stability and growth-inhibitory activity of Pt(IV) complexes. *Journal of Cancer Research and Clinical Oncology.* **1999,** *125*, 690-696.

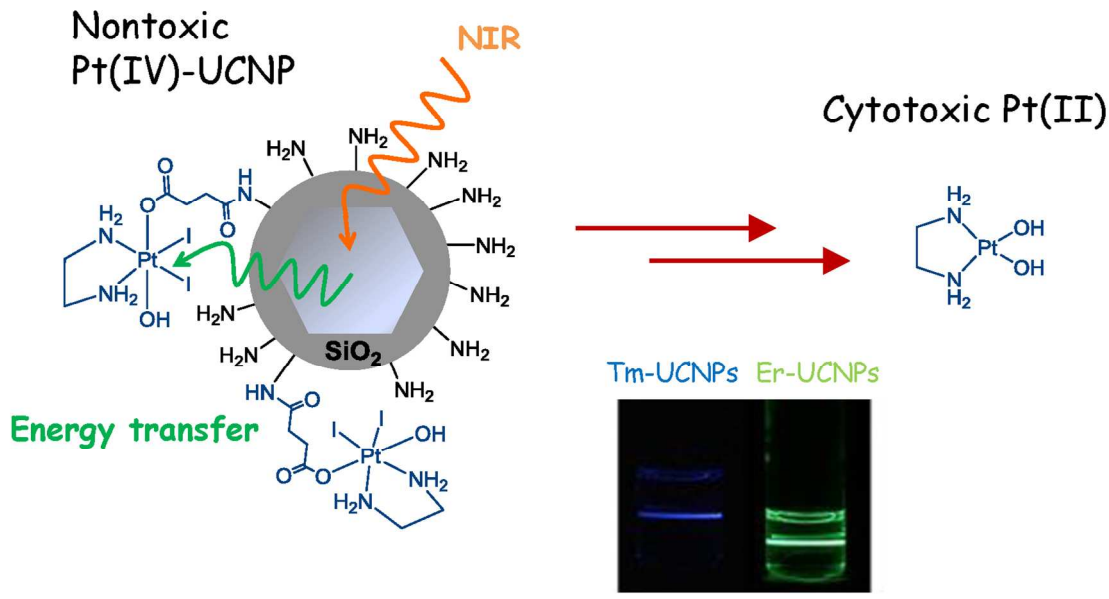

Light-sensitive diiodido-Pt(IV) prodrugs coupled with upconverting-nanoparticles (UCNP) and activated by a near infrared (NIR) light release a cytotoxic Pt(II) diamine that bind irreversibly to DNA.